RAPIDLY DEPLOYABLE LOW COST TRAFFIC DATA AND VIDEO COLLECTION DEVICE

A THESIS

SUBMITTED TO THE FACULTY OF THE GRADUATE SCHOOL OF THE UNIVERSITY OF MINNESOTA

BY

JORY ANDREW SCHWACH

IN PARTIAL FULFILLMENT OF THE REQUREMENTS FOR THE DEGREE OF MASTER OF SCIENCE

DECEMBER 2009

Acknowledgements

I would like to express my deep and sincere gratitude to my adviser, Professor Panos G. Michalopoulos Ph.D, Department of Civil Engineering, University of Minnesota, Twin Cities, whose selfless guidance, logical knowledge and unending support truly epitomizes the exemplary leadership at the University of Minnesota.

I would like to extend my gratitude to Ted Morris whose assistance and constructive comments throughout the research process was both inspiring and essential to my work.

I would like to acknowledge other individuals and organizations, which made my research possible. Research was funded by the Intelligent Transportation Systems Institute, affiliated with the University of Minnesota's Center for Transportation Studies (CTS). Financial support was provided by the United States Department of Transportation's Research and Innovative Technologies Administration (RITA) University Transportation Centers (UTC) program.

Dedication

I would like to dedicate this thesis to my parents, Barry Jay and Tina Sue Schwach, whose strong family foundation and continued dedication towards supporting education inspired me to broaden my scope of understanding and helped me to cultivate this thesis.

Abstract

Transportation practitioners, planners and researchers lack the availability of an easily deployable, non-intrusive, portable, low-cost device for traffic data collection and video recording at intersections and arterials as well as temporary remote surveillance. The necessary data usually includes volumes, speeds, classification, turning movements, queue size and length, conflicting movements, time headways and vehicle delay. They also include recording of traffic characteristics, accidents and other special situations. A visual record of traffic characteristics at intersections, arterials, or other locations can also be used for extensive analysis and research leading to improved safety and control practices. In this thesis, the development and demonstration of a low-cost, practical, rapidly deployable video recording and data collection device is presented along with the design, deployment, and data extraction process. Its major advantage at intersections is that only one unit can cover an entire intersection up to 5 lanes per incoming approach wide (20 incoming lanes total), which should be sufficient for the overwhelming majority of intersections. In addition it has the potential of extracting turning movements automatically including optional lanes through advanced machine vision or radar sensors.

Table of Contents

List of Tables

List of Figures

A. Introduction

This thesis is aimed at demonstrating a low cost, non-intrusive, portable and easily deployed traffic data and video collection device. Our focus is the acquisition of basic traffic information necessary in data collection for signal timing optimization. Such data collection primarily involves tedious, intensive and unregulated manual labor, which is undoubtedly error prone and expensive. The current standards used for performance monitoring and, signal optimization is rarely carried out and fails to meet the needs of transportation officials, but more importantly drivers and passengers. In response, our research has found the most optimal device must be capable of supplying both scheduled video and verifiable data for optimization of signal timing.

The economic costs because of inefficiencies are well documented [1]. Currently, few intersections are instrumented with sensors to collect some of the aforementioned data—in particular, traffic volumes. Temporary counting and classification devices have severe limitations, in that the data they can extract are usually constrained to point measurements of volume, speed and classification. Furthermore, they suffer from the difficulty in installation as they are intrusive, requiring interruption of traffic flow and have inherent safety concerns. Thus, most required data collection for signal optimization is typically performed manually and is therefore of uncertain quality and accuracy not to mention without methods of data verification. Cost and time considerations are overlooked at a small fraction of intersections, which are instrumented with sensors for collecting traffic data such as volumes, speeds and classification. The currently deployed sensors for collecting such information are expensive, permanent, intrusive and difficult to deploy.

Cost aside, intrusive systems such as embedded sensors and temporary counting and classification devices such as loops have their benefits, however, the safety and disruptive nature of their installation continues to make them a poor choice for gathering regularly collected data. Furthermore, since the data they can extract is usually constrained to point measurements of volume, speed and classification which needs to be collected at all

arterials on a much more frequent basis, such data collection is often is not performed and historical records for important studies at major arterials or corridors is generally lacking.

Recently introduced non-intrusive systems such as LIDAR and radar are used in permanent installations and although they are suitable for portable traffic data collection they have not as yet been packaged for this application due to cost and integration limitations.

It is worth noting that existing data collection devices have no surveillance or video recording capabilities for visual observations and verification. In short, the need for inexpensive, portable, rapidly deployable, easy to use devices for traffic data collection including for use with signal optimization that can be used on demand has been well established among practitioners as well as researchers.

Responding to the needs of transportation officials and also meeting data collection requirements we are presenting an option that considers price, occlusion and obstruction with very simple portable deployment. Desired specifications as well as the prototype design used at several urban intersection test sites and two arterial sites as a means of field deployment for data collection are also presented here along with accuracy of volumes, speeds, classification and queue length test results.

B. Background

There are several methods through which vehicle counts for signal optimization are currently obtained such as traditional manual counting [2], and tube counting or less common acoustic or radar and machine vision counting. Manual counting is generally assisted using a push button interface device to register and record each passing vehicle (for example, JAMAR Manual counter DB-400). While each counting device costs are modest, there is a recurring cost of manual counting, which is a time consuming and costly logistical process, especially when the recording period is long and/or the number of intersections is large. Furthermore, the accuracy of the recorded measurements from manual counting is difficult to verify without visual records.

Tubular counters such as the JAMAR Trax series record vehicle counts through air pulses sent through rubber tubes mounted on the roadway. The JAMAR Trax system currently costs between three and five thousand dollars but has only a small recurring cost of setup and tube replacement. Tubular vehicle counting is relatively inexpensive and accurate, however, it has drawbacks such as intrusive setup, an inability to detect turning movements, heavy vehicles breaking the tubes and a theft prone design; in addition it has no video recording and verification capabilities. Due to limitations in advanced data collection ability and furthermore, inabilities for tubular counters to be non-intrusive, tubular counters are not tested in this study.

Acoustic counting is inaccurate leading to radar counting as a better alternative. Both use a technology similar to sonar, which sends out pulses of sound and then collects the variation in each returning pulse to detect objects in the range. Another such technology is Light Detection And Ranging (LIDAR), which is an optical remote sensing technology that measures properties of scattered light to find range and other information of a target. While radar and LIDAR can be accurate methods of vehicle detection and are non-intrusive, both have limited use as they, like tubular counters, only detect a single location on the roadway and thus can only potentially collect volume, speed and classification data with no turning movement collection option. LIDAR units are new and thus no commercially available vehicle counting sensor readily exists. Furthermore,

LIDAR is very expensive and cannot detect vehicle movements throughout an area as large as an intersection and thus have no applicability in this study. Similar to LIDAR, radar's suitability and use at intersections has not been established, radar, like LIDAR has no potential for collecting an entire intersection from a single location or with a single unit thus creating a deployment cost far exceeding that of other sensors. Radar counters such as the remote traffic microwave sensor (RTMS) presently cost between four and five thousand dollars and require a more complex integration aspect for deployment than other existing devices such as machine vision. In addition, with the goals of signal optimization in mind a deployment of a basic counting device would not be suitable for testing with this device. Due to cost and more importantly utility limitations for advanced data collection with the portable system being designed and tested in this thesis, LIDAR, radar and acoustic counters were not tested.

Machine vision technology utilizes image-based camera sensors in order to detect vehicles in real-time or by post-processing the video. This technology has the greatest potential since camera sensors are ubiquitous and cost effective as they have the capability of detecting several different traffic measurements at multiple locations within the road facility with a single sensor (speeds, counts, headways, etc.). Furthermore, they are non-intrusive, and, capable of providing visual records for verification and storage. Like RTMS, most commercially available machine vision systems are designed primarily for traffic management rather than as an 'off-line' traffic measurement and analysis tool [1]. Their cost is comparable or lower than RTMS. A review on these and similar commercially available non-intrusive traffic measurement sensors may be found in [2] and [3].

Based on such considerations and its versatility (which includes a number of new detection-types and Boolean logic detection logic) video sensors are most suitable for non-intrusive portable data collection at intersections. While a few experimental portable, image-based, traffic measurement systems have been developed [4], none is commercially available. In addition there is a liberal interpretation regarding the usage of the term 'portable' in the literature. For the purposes of this thesis, we evaluate the degree of portability by the ability to move, assemble power, configure, or disassemble the

system within a short time period, in the order of 15 minutes or less. This is because if the period were longer, the ease of setup and portability would be compromised. In terms of the latter, one adult should be able to carry out the entire deployment process alone without the assistance of lifting machinery. Finally in terms of simplicity, operation of the system should require little training in the order of 4 hours or less.

Non-intrusive traffic measurement infers that vehicular traffic is not disrupted during installation or removal. This means that safety is never compromised during the deployment process. Furthermore, portable systems must be capable of unattended operation for extended periods. Previously developed video based systems are basically one-of-a-kind and tend to be trailer-based extendable pole mast systems with battery storage (and possibly solar array apparatus). The pole mast sections foldout to various configurations for allowing detection equipment to be erected [5].

Another approach used for intersection traffic data analysis and surveillance consists of a van equipped with rooftop mast. In this configuration the camera, machine vision processing, transmission, and recording components are located inside the vehicle (4). Such a 'drive and park' deployment system contains readily available power from the vehicle along with ample storage; this represents a complete 'mobile laboratory' rather than a low cost data collection device. A site-based permanent camera was necessary to collect video data under inclement conditions such as rain or snow. Using this setup the feasibility of extracting turning and thru lane counts at urban intersections using either a previous commercially available strip-region based video tracking algorithm or a commercial tripwire video detection machine vision system was assessed. The measurement accuracy of the turning movement tripwire technique developed was too complex and not sufficient to be used in practice at larger intersections. Conversely, the tracking algorithm produced accurate measurements but was too difficult and cumbersome to configure. Nevertheless, the ability to record and extract all required data on site was successfully demonstrated. The cost of this van system was approximately $100,000 dollars. Arguably the degree of portability for this and other trailer-based systems is limited because of the difficulties securing and positioning them at urban

streets as well as rapidly deploying them at multiple intersections. Furthermore, parking at distances far from the intersection requires increasing mast height for placing cameras.

Recently a portable system was developed and deployed on high-rise building rooftops along a 1.5 mile long freeway 'commons' site in Minneapolis for digitally recording live accidents while simultaneously extracting traffic data in order to study accident dynamics [6]. This system consists of one or more commercial machine vision sensors (Autoscope) and manual, vari-focal video cameras affixed to a 6' pole mast. The base of the pole mast consists of a 3.5x3.5 ft^2 weighted platform (250 lbs) and a 2'x 2'x 2' environmentally controlled enclosure. The system provides real-time collection, storage, and transmission of vehicle headways, speeds, length classification, and volume counts generated by the Autoscope video sensor as well as storing MPEG4 encoded video (DivX v.5.1) [6]. The video recording and transmission is implemented on a small footprint (MicroITX) PC. Other off the shelf media conversion hardware connects the PC and machine vision sensors to an 802.16 30 mbps 2-way radio, which wirelessly transmits all data back to a remote location for further post processing and analysis. Laboratory experiments revealed that the power consumption from the machine vision sensor and communications hardware was approximately 30 Watts (PC and camera-hardware temperature control was not considered). External power was readily available at each site. Current traffic measurements for such a system were based on Autoscope's data extraction system. The accuracies are acceptable and in accordance with the hardware's operational parameters. Although some of the design and deployment aspects of this portable system provide important relevant information, this system is not deployable for all practical purposes at intersections as it lacks easy camera installation, weatherization and autonomy. Furthermore, the cost is relatively high ($15,000) but without stand alone features such as power, cabinet, camera pole, etc.

'Hand-erected' extendable mast designs supporting side-fire radar traffic counting and speed sensors powered by deep cycle batteries also recently developed [7]. The pole systems with a side-fire radar sensor (RDMS) cost approximately $6,000, are easily stored, and can be quickly transported to multiple sites (sensor faces at a 90 degree angle to the traffic flow). The mast is mounted on existing infrastructure. A deep cycle battery

can enable the RDMS to collect data for approximately three days. Although this system is the most space saving and least intrusive of all previously mentioned systems, the system has no surveillance or video recording capabilities. In addition, the radar sensors tested are not suitable for detecting stopped vehicles, queues, and turning movements; i.e. not suitable for intersections.

A myriad of work-zone intelligent transportation systems (WZITS) have been developed as a safety countermeasure to warn drivers of dangerous traffic conditions. Unfortunately, the effectiveness of a WZTIS is diminished if the actual traffic flow conditions do not correspond with the sensor information leading to false warnings; these confuse drivers and reduce the credibility of the system, which is often ignored. This can lead to situations where drivers crash into work zone areas because they are unprepared to stop. Such 'dangerous' traffic conditions are typically characterized by unpredictable queue formations, which propagate rapidly into higher speed traffic immediately upstream from the active work-zone. 'False positive' or missed warnings could be reduced if the location of queue tails in addition to vehicle speeds in proximity to the active work-zone can be accurately detected. In this test, low-cost rapidly deployable and portable queue detection WZIT warning system is tested. Timely and reliable wide area queue detection will be achieved through enhancements to a previously developed easily deployable, non-intrusive, portable, low-cost machine vision based device for wide area detection, and traffic data collection. To demonstrate WZITS feasibility, the queue detection data will be wirelessly transmitted to a remote upstream location for triggering roadside emergency warning devices (such as VMS, flashers, etc…).

The likelihood of an increase rate of crashes at work-zones has been well recognized over the years. A recent study from Bai & Li in 2006 reported that driver errors caused 92% of the fatal work-zone crashes in the past thirteen years [8]. The most common driver errors include inattention, disregarded traffic controls, speeding, and alcohol impairment. According to their analysis, most Kansas fatal work-zone crashes (67%) during 1992 and 2004 occurred on non-intersections of the highways, and 19% were intersection related [8]. Field studies by Fontaine in 2003 determined that WZITS are most effective in areas where queue lengths as well as speeds are variable throughout the day [9]. Further, Wang

in 2003 noted that crashes, significantly many rear-end collisions, are attributed from preceding vehicles rapidly reducing their speeds (e.g., shock waves) [10]. Essentially, there is a 'grey zone' containing a transition point between rapidly forming queues and vehicles traveling the posted speed limit upstream of the work-zone. Unfortunately the speed of such queue tail movements precludes manual intervention by a traffic controller [11].

Many WZITS implementations today comprise the use of Doppler Radar units, or in some instances infrared 'trip-wires', or machine vision to detect vehicle speeds and presence. All such systems measure vehicle speed at different locations upstream of the work-zone. The speed measurements are then categorized into meaningful warning levels that are conveyed to drivers (Variable Message Sign (VMS), triggered light flashers, HARN, etc.). For example, the Minnesota Department of Transportation (Mn/DOT) deployed a several skid-trailer 'nodes' with machine vision systems or radar units along several upstream locations of work-zone sights. Wireless communication was used to relay warning messages (e.g., 'slow speeds ahead', etc.) to a portable VMS. Results of the field evaluations for this system indicated a significant reduction in speeds through the work-zone area when the WZITS was in use. The cost of each node was $78,000. Tudor and Lorie in 2003 also deployed a similar system in Arkansas [12]. The cost of their system (subtracting the $60,000 for the HARN system), was $263,000 and consisted of Doppler Radar speed stations integrated with a VMS, plus an additional stand alone portable VMS sign. The stations were deployed approximately 3.5 miles from the work-zone taper while the individual VMS was situated seven to twelve miles upstream of the work-zone. Vehicle related crash fatalities decreased from 3.4/3.2 per 100 million miles traveled to 2.2 per 100 million miles traveled over the course of the deployment (1 year) [12].

Recently, in 2005, Sullivan proposed a rapidly deployable WTITS that consist of 'smart-barrels' [13]. Without going into great detail, the essence of the system would be to 'track' the tail of queues by detecting a 'rapid' reduction of vehicle speed along several regularly spaced points up to about ¼ mile upstream of the work-zone. The system as a whole was never actually deployed although driving simulation experiments were

conducted to ‘test’ the system under several controlled scenarios. The results of that study indicated significant speed reduction amongst subject [13]. Therefore, queue length propagation into upstream traffic without sufficient warning to drivers is recognized to increase accident risk near work-zone areas. In addition, the need to accurately detect queues with easily deployable, cost effective WTITS has been recognized by others.

In conclusion, although aspects of each of the designs and experiments provide useful knowledge to guide the rationale for the prototype design and development, none of the previous efforts have fully addressed all of the aforementioned concerns including; cost, intrusiveness, portability, reliability, performance and traffic data collection. In light of this, the functional specifications and thus the remainder of this thesis are specifically tailored to address and mitigate these and other concerns voiced by transportation practitioners we consulted.

C. Functional Specifications

Before exploring design alternatives for the apparatus, we developed through a series of meetings with transportation engineers at the University of Minnesota and traffic engineers from the Minnesota Department of Transportation (Mn/DOT) a set of specifications for our apparatus. Functional specifications related to size, weight, durability, portability, and data collection capabilities were essential in the development of the device. Such specifications are governed by minimum capabilities that should result in a useful system as well as ideal specifications, which significantly advance state-of-the-practice for traffic measurements at urban intersections and mid block locations. The specifications are defined by nine criteria:

1. Traffic data collection and measurement	**6.** Data organization format
2. Volume and geometic limitations	**7.** Setup and portability
3. Speed	**8.** Environmental conditions
4. Classification level	**9.** Cost.
5. Time periods and scheduling	

Such specifications were developed and presented to local traffic consultants with Professional Engineering certification and Mn/DOT technicians involved with regular vehicle data collection, for review and comment prior to the design stage and are described below as well as studying requirements within the Minnesota Manual on Uniform Traffic Control Devices (2005) [14].

Traffic Data Collection And Measurement Specifications

- All standard traffic measurements such as volume, classifications and speed must be collected at the lane level.

It is desirable for the apparatus to at least have the ability to extract turnings at intersections.

Volume And Geometric Limitations

- The accuracy range for volume counts must be at least 85% and preferably, 95% of actual.

The above specification is standard practice.

- The system should be able to handle road widths up to eight lanes or up to 100 feet. Therefore, the system must be able to handle up to eight lane arterials or intersection approaches up to eight lanes total including any and all turning lanes. Subject to the 100 feet limitation, the system should have the capability to handle isolated turning lanes separated by a median.

The prevailing maximum number of lanes on arterials in Minnesota is eight lanes. This means that if a median is included the maximum road width should be 100 feet.

- The system should be able to handle up to four intersection approaches simultaneously.

This is due to time and cost considerations as well as efficiency since the user should not have to replicate the installation at the same site. When conditions do not allow, it is desirable to collect at least two approaches such that no more than two installations are necessary at a given site.

Mn/DOT frequently is required to collect per-lane volumes for arterials, which contain four lanes in each direction. This is because these arterials carry high volumes of traffic, which significantly impacts demand patterns on Freeways and other highway facilities. For example, Mn/DOT's portable detection system uses a side-fire Remote Traffic Microwave Sensor radar system (RTMS) [15] collects total intersection volume and per-lane volume counts for up to four lane roads (although product literature for this device will claim the device can measure up to 8 lanes). The

minimum, and perhaps more feasible, number of lanes at either intersection or mid-block locations are four lanes; as previously noted, other portable measurement systems achieve this in practice. The system should have the capability to simultaneously count isolated near right turn lanes; such traffic data are necessary in order to better assess alternative intersection designs. Note that intersections of interest to practioners with fewer than four approaches have been identified for our study.

A desirable road width distance of one hundred feet for either median or non-median separated intersections or mid block locations was indicated in order to observe traffic flows in up to 8 lanes (assumes lanes are standard 12' lanes). Lastly, if it is not possible to cover all intersection approaches simultaneously, it is desirable to at least cover two approaches. For example, if traffic characteristics for only two approaches for a 4-approach intersection can be observed and measured, then two systems could be deployed to capture all approaches simultaneously (dependent on cost and transportability considerations discussed below).

Speed

- The speed accuracy is only needed at midblock locations with minimum required mean accuracy of 90 percent.

Vehicular traffic speeds located within the intersection is of little value to practitioners in so far as these measurements have little impact on assessing demands and travel behaviors. However, speed measurements are occasionally collected at mid-block locations before intersections. The current portable traffic measurement data collection system utilized by Mn/DOT has the capability to measure and aggregate vehicle speeds as long as vehicle speeds are traveling more than 5 miles per hour.

Classification Level

- Vehicle classification must include at least three classes for passenger vehicles, trucks and buses. The mean accuracy should be no less than 85 percent.

Here, Buses and semi-tractor-trailers are both of the same class while trucks such as municipal vehicles are of a separate class. Data classifications, which would comply with FHWA thirteen classes, would be desirable particularly for mid-block location traffic measurements [16]. Note that the thirteen classifications are stratified by number of axles and the length between each axle. In practice, due to time constraints and the difficulty in distinguishing all 13 classes, typically no more than 5 classes are obtained during temporary field site data traffic data collection efforts. For intersections 5 classes is more than sufficient for most studies. Autoscope, a commercially available video processing system and the device used in this study, is capable of delineating five class types based on vehicle length.

Time Periods And Scheduling

- The standard traffic measurements require sampling periods must be user specified to one of the following: 1 minute, 5 minute, 15 minute, 1 hour, or daily (24 hour) increments.

Based on historical records for traffic warrants used for signal retiming [17], a 15-minute interval was selected to be the standard for all data counts in this study.

The system must be able to be deployed in the field and operational (for scheduled recordings) for at least a month during which it must be able to record at least 48 total hours of scheduled video and data without power, memory or other maintenance.

Based on discussion with traffic practioners, 48 hours of total video is to be considered a practical lower bound capability of the system. A desirable recording schedule for signal re-timing would consist of eight hours per day broken into three scheduled peak period (see time periods below) then a minimum of six days are needed to meet the 48 hours of required data collection. Ideally, practioners voiced a desire to have two weeks of deployment over which, recording and data collection

would take place mid week (Tuesday, Wednesday, Thursday) during only peak hours as follows: 6:30 – 9:30AM, 11:00AM-1:00PM, and 3:30-6:30PM.

Another goal voiced by practioners is to measure, without revisiting the test site, the beginning/end week conditions (Monday/Friday), or quantify non-peak conditions. For example, the Minnesota Department of Transportation (Mn/DOT) will occasionally collect traffic volume data during off-peak periods over a 24 to 48 hours period. In conclusion, the system must have the ability for a myriad of user-scheduling and sampling periods for all standard traffic measurements under consideration. This also applies to advanced traffic measurements, such as vehicle delay and turning counts) as well.

Data Organization Format

- The system should produce data in a standard presentation format.

The most desired format is a table, which collates all data row-wise; into the desired time period (5 minute, 15 minute, etc.) for each approach (or lane) and in each direction (columns). From these data other aggregate measurements can be tabulated such as: hourly/daily measurements on a per-approach (or lane) or summated approach (or lane) basis.

Set up And Portability

- The system should be compact and lightweight with a footprint measuring no more than 2’ x 1.5’.
- The system should be storable in a standard size mini-van.

Since the minimum sidewalk clearance between signal poles and the edge of the sidewalk is five feet, a maximum are footprint for the apparatus should not exceed 2 x 1.5 feet in order to ensure adequate clearance for wheelchairs as well as pedestrians. Total dimensional specifications are critical for hauling multiple systems in a

practioner's vehicle and storage of multiple systems within such vehicles will be required for wider scale deployment across multiple intersections.

- The system should be cartable by a single person and deployable within fifteen minutes with no part weighing more than 60 lbs.

The apparatus should be easily transportable in vehicles such as minivans and cargo vans. A general capability voiced by field engineers is that the apparatus should easily disassemble in order to maximize storage efficiency both at base facilities and within the vehicle. For example, the maximum cargo length of a stock Dodge Caravan is reported to 8 feet in length, with a maximum width of 47.5 inches, and a maximum height of 39.5 inches. This includes a total cargo capacity of 144.2 cubic feet. Other similar vehicles were checked; for example, the Toyota Sienna maximum length is 6.5 feet (which was the minimum of all the vans checked) whereas a typical cargo van has a cargo capacity of 12 feet by 4 feet by 4 feet.

It is assumed that all field sites will have some infrastructure (sign, signal, or light poles) for the apparatus to be affixed. An acceptable complete set up time of no more than fifteen minutes was determined; anything longer will nullify its utility especially for very short studies where only a few hours of data are needed. A desirable weight for the total system is 75 lbs. Or, at least, individual components, which can be quickly transported to the field site on-foot, should be less than this weight.

There should not be any exposed power or communication cables. No other external power supplies should be required to operate the system for various time periods discussed above. If additional power via batteries needs to be replaced or added, there should be no interruption in the data collection at the site. Furthermore, available power should be managed as efficiently as possible and conserved during times of system idling where no data collection is taking place.

Video imaging vehicle detection accuracy will improve as camera height is increased within the range of 20 to 40 ft above the roadway. The highest camera height seen for minimizing cross-lane occlusion was 38 feet for adjacent lanes, and 150-foot downlane approach distances [18]. Large intersections with more than 4 lanes per

direction may still require multiple cameras, thus height restraints can remain within the 28 ft minimum parameter, which was obtained with the modified apparatus. It is worth noting here that while multiple cameras at a single intersection would be ideal, cost and integration limitations are such that only a single camera is required for this system.

Environmental Conditions

- The system should be of industrial quality and able to stand adverse weather including winds up to 70 mph, hail, snow, rain, sleet, humidity and extreme cold and heat.

The desired minimum survivability wind load characteristics should be at least 70 mph, which are structural design constraints used by Mn/DOT for their signal and light pole designs and in correspondence with Mn/DOT field engineers. The desirable environmental range for operability during data collection should equal commercially available video-based traffic detection systems published from other video-based traffic sensing systems. For example, the Autoscope Terra has an operable temperature/humidity operational range from -29 degrees Fahrenheit to 140 degrees Fahrenheit at 100% relative humidity per MIL-E 5400T paragraph 4.3.24.4. The system should operate under day/nighttime lighting conditions. However, initially, there is no need for field collection during heavy snow or precipitation.

Cost

- The total system building costs including hardware, software and labor cannot exceed $8,000.

Practitioners present at our panel meetings voiced that a total cost of approximately $8,000 dollars per system including both software and hardware would be acceptable. Other portable traffic measurement systems that were previously deployed were similar in cost [19].

D. Prototype Design and Deployment Procedure

In this section, the prototype design and deployment procedure are discussed. In order to fully understand the components and necessary areas of focus for the design and implementation process and furthermore, to minimize issues encountered during these processes, an initial field test was completed by modifying an existing apparatus [19] to collect initial field test video data. This will be described next. Then the subsequent design of the prototype developed for this study will be described. Based on the prototype design, the steps required to deploy the system will be summarized.

The apparatus was primarily designed to deploy side-fire radar sensors at an approximate height of 17 feet above the road surface. This was achieved by coupling two eight-foot length aluminum poles. From the field tests, in addition to geometric and occlusion analysis [20] we determined that a desirable minimum elevation height of 28 feet for the cameras is required. This was achieved by adding an additional 8' pole section using an identical coupler and modifying the sensor mounting bracket to hold a video camera. The base of the mast was then mounted to a signal pole approximately four feet above the sidewalk. The pole base mount was hinged to act as a fulcrum to lift the mast the mast into vertical position.

The field test device was very primitive and supplied insight as to the needs of a more industrial system. The initial deployment of the existing apparatus required constant supervision and weighted heavily upon existing infrastructure. In addition, hoisting the mast into the vertical position proved to be more difficult than anticipated due to the counter acting torque of the pole weight. This created some safety concerns because hoisting the mast in this manner often interfered with pedestrians or vehicles passing underneath. Nevertheless, three hours of video recording were obtained from the testing and the recorded video was then analyzed to determine the needs of our prototype including quality of the recorded video and durability of the pole and apparatus as a whole.

Based on this initial field test it was clear that to design such a system the limiting factors are constrained by cost, size, weight, stability, and data recording functionality. The resulting system which meets our functional specifications, cost $7800 to construct. Due to conflict with University policy regarding intellectual property rights, a more itemized cost breakdown is not available at this time. The system digitally records MPEG4 video from the camera upwards of 45 hours without power or data storage replacement. The system base box is a NEMA-4 enclosure with a footprint of 24 inches in height by 20 inches length by 12 inches deep. It was built from off the shelf components with custom machined parts added as necessary. A self-raising mast with internal cables elevates the 640x480 CCD video camera between 28 to 30 feet above the pavement surface (Figures 1 & 2). The components in the box are the DVR computer, the power management microprocessor, and the deep cycle batteries, which contained no moving parts for optimal utilization in the field (Figures 3 & 4). Software for the DVR and microprocessor were built upon open source software.

It was desired to have multiple cameras recording from a single apparatus; however, cost and size limitations prevented the implementation of multiple cameras. In order for a second camera to be implemented into the apparatus the following additions would have been needed: a larger mast which would support the additional weight and wiring, a second camera and DVR for recording and processing the second video stream and additional batteries to handle the increase in power consumption. The mast cost alone in order to house multiple cameras and wiring was not possible without exceeding out budget limitation, however, additionally a second camera and DVR would have required additional funds and power and thus a larger NEMA box would have been needed to house the additional batteries and was not possible within our size limitations. For all of these reasons the implementation of multiple cameras was not an option for this system.

Figure 1: System deployed at Site 4.

Figure 2: The cabinet with mounted components.

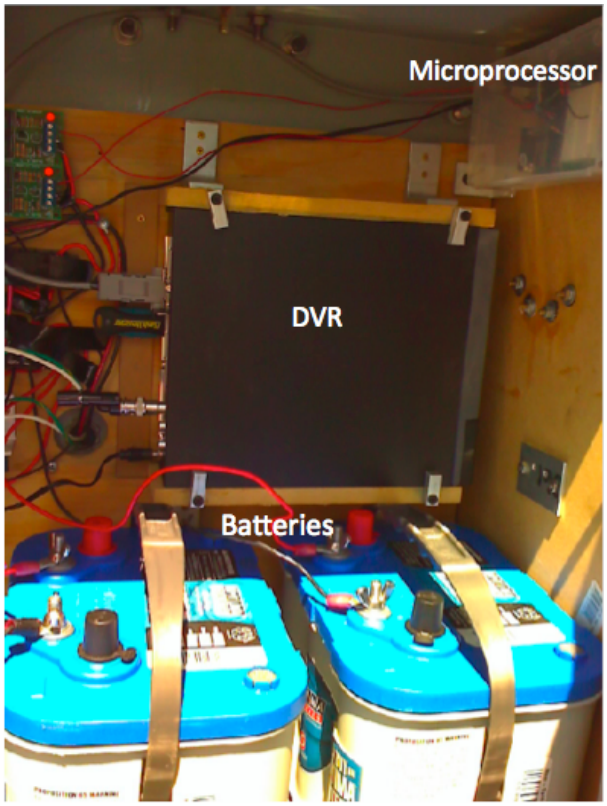

Figure 3: Inside of cabinet (batteries, DVR and microprocessor).

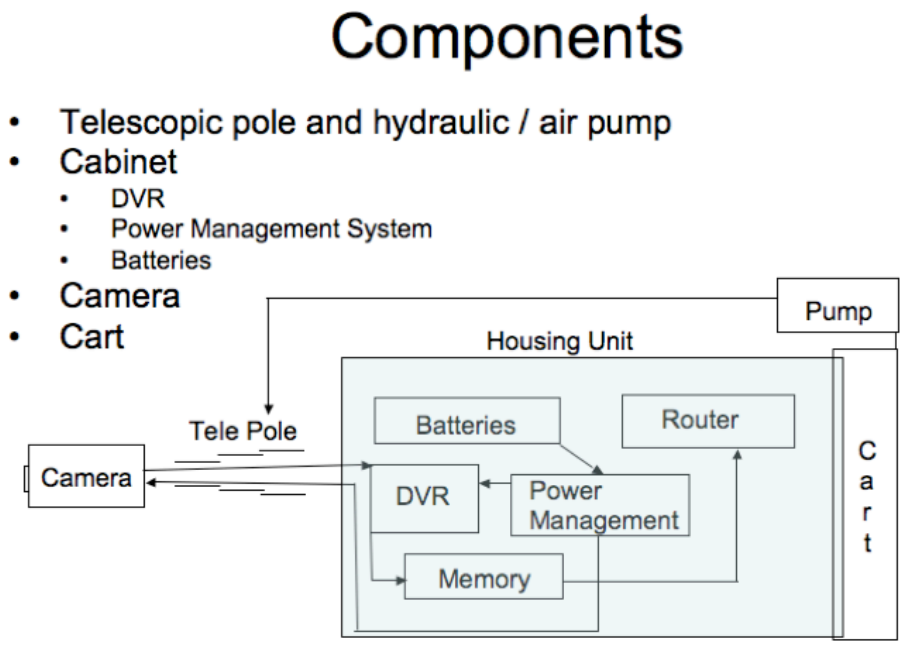

Figure 4: Diagram of components organization.

The deployment procedure is organized into 12 steps. This deployment process is performed in reverse order to remove the system from the site. It should be noted that at present twisting the pole before it is locked into place achieves pan adjustments. Table 1 describes the set up deployment procedure for the current apparatus.

Table 1: Apparatus deployment procedure.

Steps	Apparatus Deployment Procedure
1) Unload Base	The base box is placed upright on the sidewalk or other stable hard surface.
2) Elevate Base	The base box is elevated allowing the trolley frame to roll underneath by lowering the base legs.
3) Latch Base to Trolley	The base box is latched to the trolley with buckles located on the left and right sides of the box.
4) Mobilize Base	The legs are elevated and trolley wheels locked.
5) Attach Batteries	The batteries are placed in the base box.
6) Attach Camera and Pole to Base	The camera mount is latched to the top of the mast (if removed for transport) and the pole is slipped into the base mount of the base-box.
7) Transport Apparatus to Test Location	The wheels are unlocked and the entire system is wheeled to the appropriate location at the site which point it is backed up to the pole at which point the wheels are then re-locked.
8) Mounting Bracket	The pole mounting attachment described earlier is adjusted, fastened and secured to the site infrastructure.

9) Remove Cart from Base	The wheel mounts are removed while the feet are lowered lifting the box off of the cart as which point the cart is removed.
10) Raise Mast	The mast is then raised with a battery or hand powered air pump.
11) Power System	The system is then powered and booted with the appropriate options set.
12) Lock Apparatus and Exit	The box is padlocked at the front, back and top door and the cart is wheeled back to the storage location.

A group of five students were asked to deploy the apparatus to validate the deployment time constraint of 15 minutes. After a 30 minute training session each was asked to deploy the apparatus without assistance. Each student was successfully able to deploy the apparatus without assistance in under 15 minutes for setup and well as 15 minutes for removal. The average setup and removal time was 11:42 and 8:51 respectively.

E. Test Site Selection And Data Collection

In this section a background of historical data collections, environmental factors and approach topologies preface how test site selection and data collection are coordinate. It is important to remember that the main objective of the video recordings is to obtain accurate traffic data from recorded video observations. Another objective is to evaluate automated extraction, as a means to equal or surpass manual counts and reduce the time and effort required. Part of this evaluation requires analyzing the factors that affected the automated extracted traffic measurements. Such factors, which affect manual and automated traffic data extraction from the video, have been categorized as controllable or uncontrollable [21]. The traffic characteristics (traffic volumes, classes, etc.) wind, weather, and environment lighting are uncontrollable factors. Camera location is controllable to some extent however for a myriad of practical reasons very rarely can

optimal positions be achieved in real life field deployments. Therefore, during the site selection process we performed occlusion analysis to determine the proper camera placement. This is accomplished with the objective of covering an entire intersection with a single camera while still being able to evaluate video image processing for data extraction and deployment feasibility at typical intersections [20].

Table 2: Historical count data time table.

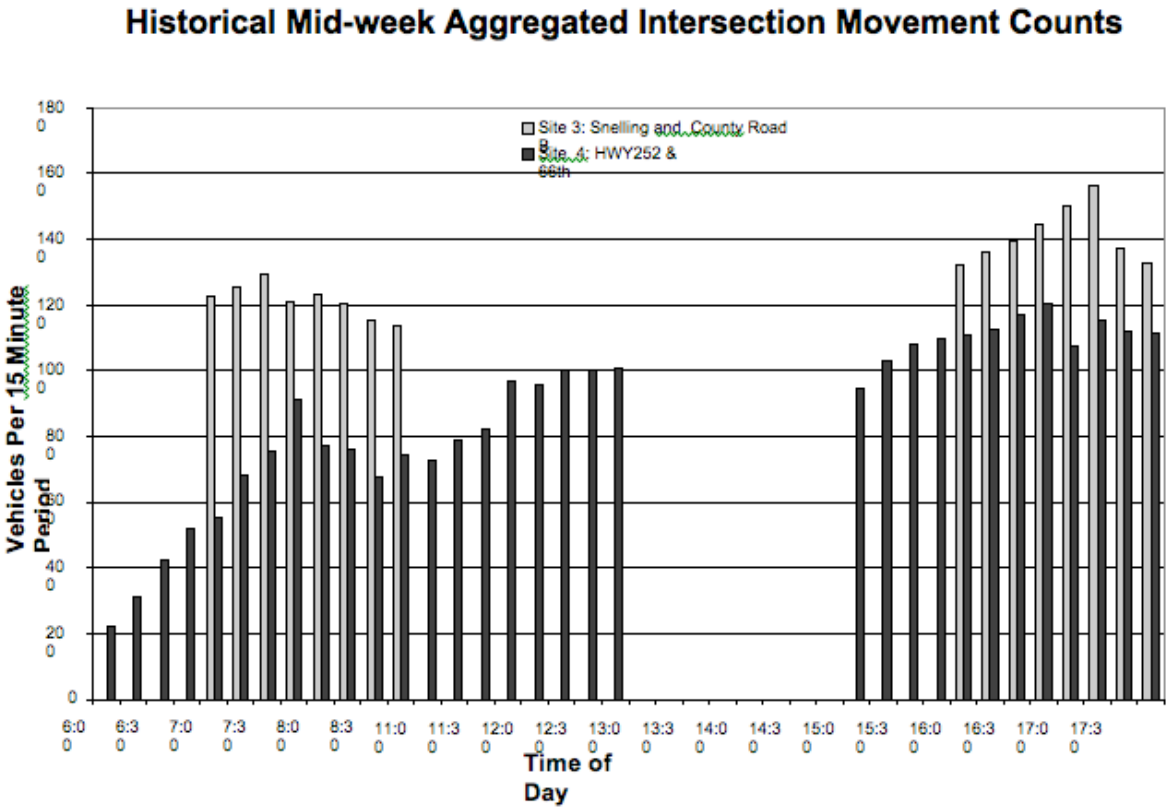

The following conditions are taken from the above historical data and recommendations from practitioners [22].

Normal Historical Collected Peaks in Minnesota Metropolitan Arterials

Tuesday: 0600 – 0845; 1500 – 1745

Wednesday: 0600 – 0845; 1500 – 1745

Thursday: 0600 – 0845; 1500 – 1745

Collection Peaks at Selected Site Arterials (based on historical and practitioner suggestion)

Weekdays: 0600 – 0900; 1100 – 1300; 1530 – 1830

Weekends: 0600 – 0900; 1100 – 1300; 1530 – 1830

Following engineering practice, three daily periods (AM, PM and off-peak) were selected. Specifically at all sites, mid-week (Tue,Wed.,Th) and weekend data were collected at three counting periods [0600-0900, 1100-1300 and 1530-1830]. A total of 106 hours were recorded and analyzed between August 2007 and May 2008 at both arterial and highway locations in the Twin Cities metropolitan area. These locations will be described in details later in this thesis. For this study automated traffic measurement extraction was not analyzed during extreme rain or poor lighting (pre-sunrise and dusk) although it should be noted that the system collected video data reliably during these time periods and was suitable for manual counting from the recorded video. Each site was selected based on requirements found in the functional specifications alongside recommendations from practitioners.

During the selected data collection periods lighting varied especially during sunrise and sunset thereby affecting counting accuracy. Sunset occurred later than 7:41PM after the time of data collection, i.e., after the PM peak period therefore no recording was necessary during or after sunset. Sunrise, however, varied between 6:53AM and 5:30 AM, while collection starts as early as 6:00 AM thus introducing lighting variation. For example, midweek data collections during the first week of April yield approximately one hour of pre-sunrise conditions. Similar effects will occur on later sites, including a post-sunset recording on Site 4. This should be a noted point in the results for understanding how light and shadows effects may hinder the results gathered from such video. In regards to the apparatus developed here, all hardware components were industrial quality; to be sure, since the initial deployment, the equipment was left unattended for data acquisition and video recording for upwards of three weeks under adverse environmental conditions such as extreme heat and cold, wind, rain, snow, and even hail without incident.

Topology

Due to the many combinations of approach design configurations at intersections and the maximum number of lanes specified (eight per approach) it is evident that a large number of intersections would be needed to satisfy testing requirements for all possible intersection designs. This is because there are fifteen common intersection approach lane configurations and commonly four approaches per intersection. Therefore, the possible intersection designs are combination 15, 4 at a time. For this reason we developed the methodology described next to minimize the number of test sites needed.

Table 3: Topological representation of urban intersection approaches.

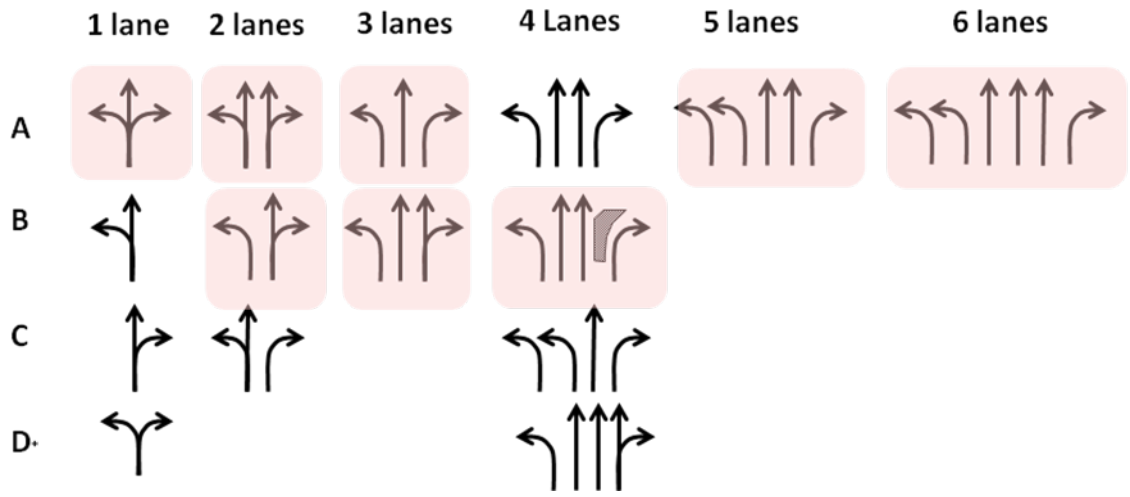

By strategically selecting intersection sites, which include typical geometric layout complexities, we ensured that the system would have the ability to accurately extract traffic measurements in the majority of intersections. This was accomplished in cooperation with transportation practitioners present at out panel meetings. Initially, we identified fifteen intersection approach types, which are prevalent within the Twin Cities metropolitan area. From the set of fifteen a topology was identified in order to reduce the number of representative intersection types, which actually needed to be selected for testing the new portable video-based traffic measurement system (Table 1). For example, if the system can successfully be used to extract traffic measurements at a single-lane

approach type A, then all subsequent single lane approach types B through D should produce results of similar accuracy. Considering type A can cover all two-lane approaches, i.e. all other two-lane approach types are similar. Finally at three-lane approaches, testing types B will cover a three-lane type A configuration.

Lane and intersection geometry may also influence measurement accuracy. For example, 5, and 6 lane topologies in Table 1 do not contain shared lane approaches, which is typical at high volume arterials. Such arterials commonly utilize dedicated turn and thru lanes. Therefore, experimentally validating a 2-lanes type B and 5-lane type A configurations will also validate 4-lane type B, C and D. Finally isolated right turn lanes represent another unique geometry not included.

Based on the above reasoning one only needs 4 test intersections consisting of only eight approach types. Through careful selection of intersection approach geometries, we were able to identify four intersections, which included the eight approach-types, which are shaded in Table 1. The approach geometries covered by each site are indicated in the right column of Table 2. We started with initial field volume data collection and video recording experiments at Site 1, which includes the shared single and two-lane approach configurations. We then progressively added lanes by collecting the same information and testing at Site 2. The effects of increasing the number of approaches shown in Table 1 were analyzed from the collected data at Sites 3 and 4.

Each of the four intersection sites will be described in detail next. In addition, a fifth and sixth arterial site will be described below. This fifth site is a mid block location used for testing the extraction of speed, classification, and volume upstream of a signalized intersection. The sixth site was used for testing a queue length detection algorithm. The apparatus was deployed for more than 700 hours for all the sites tested under a variety of weather conditions. Experimental results from the first four sites will be presented first, followed by results from the midblock and queue length traffic measurement experiments.

Table 4: Selected intersection sites and their approach geometries.

Site	Location (Main & Side)	Approaches Types
1	CSAH 5 & Ottawa Ave, Saint Louis Park	2 x 2-lanes-A, 2 x 1-lane-A
2	CSAH 5 & Louisiana Ave S, Saint Louis Park	2 x 3-lanes-A, 2 x 3-lanes-B
3	CSAH 51 and Co. Rd B., Roseville	1 x 4-lanes-B, 1 x 5-lanes-A, 2 x 3-lanes-B
4	State HWY 262 and 66th St., Brooklyn Center	5-lanes-A, 6-lanes-A, 3-lanes-A, 2-lanes-B

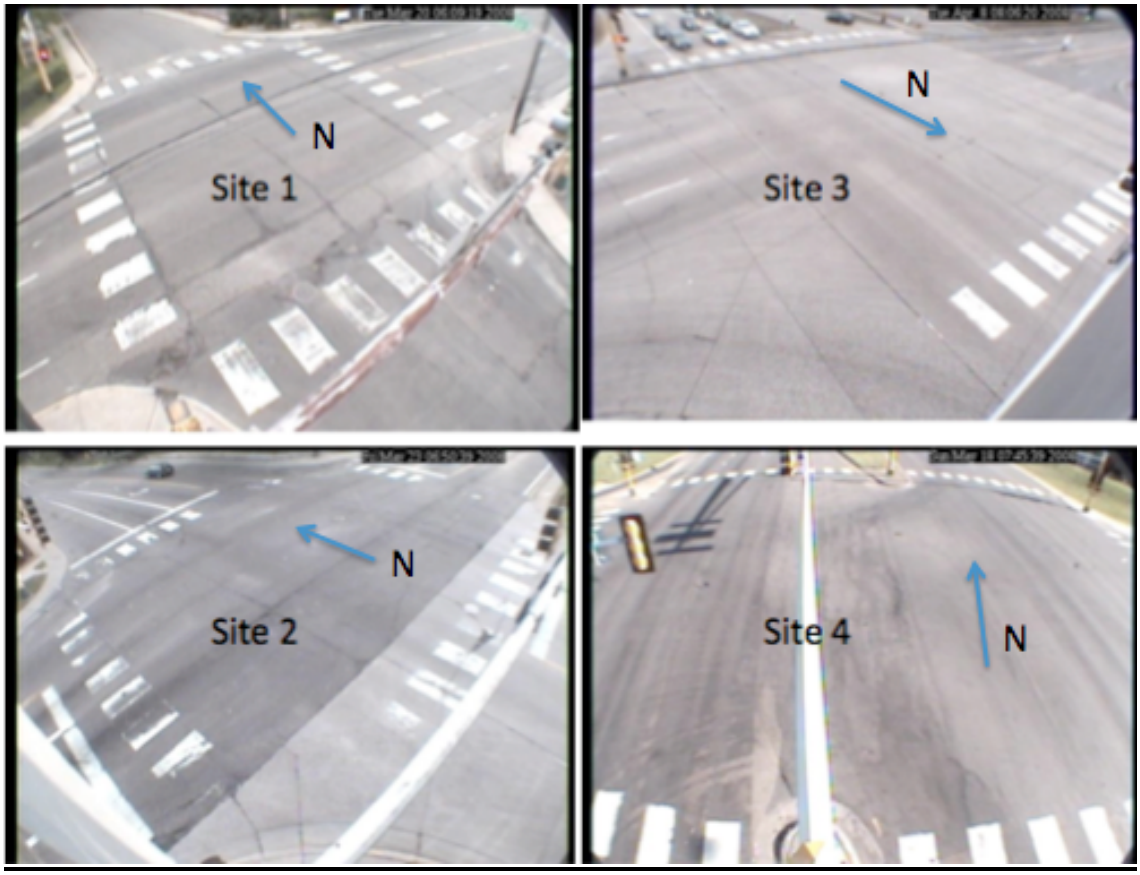

Figure 5: Selected intersection sites.

Site Descriptions

The following site descriptions breakdown and detail the test sites used in regards to site layout, areas of interest for data collection, deployment information and environmental factors experienced while on-site.

Site 1, Minnetonka Boulevard (CSAH5) and Ottawa Ave S, has two, single shared lane approaches running North and Southbound on the side street, Ottawa Ave S, and two, two lane shared approaches running East and Westbound on Minnetonka Boulevard (Figure 5). This site was used to run experiments to extract traffic measurements on single and double mixed lane traffic flows. The circled portion was associated with the largest approach count measurement errors. The system was deployed at this site for a

total of 106 hours. The weather conditions during the deployment period varied from sunny to overcast with a maximum wind speed of 16 mph.

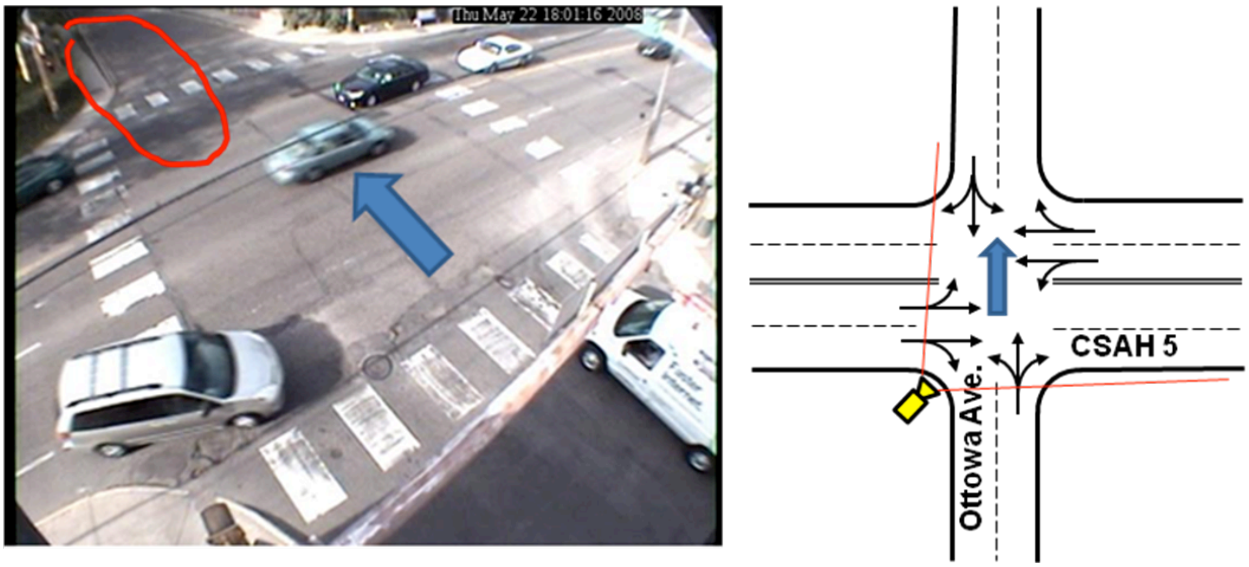

Figure 6: Site 1, apparatus camera view and layout of County HWY 5 and Ottowa Ave.

Site 2, Louisiana Ave S and County State Aid Highway 5 (Minnetonka Blvd) consist of an East and Westbound (2-lane A) with exclusive right turn pockets and a mixed straight and left turn lane as well as an East and Westbound single mixed lane for left, right or straight movements. The Northbound and Southbound approach consists of 3-lanes; an exclusive left turn lane, a middle straight only lane, and a mixed straight and right turn, right lane (Figure 6). This site was used to run experiments to extract traffic measurements on two and three lane mixed traffic flows. The system was deployed at this site for a total of 106 hours. The weather conditions during the deployment period varied from sunny to overcast with a maximum wind speed of 22 mph.

Figure 7: Site 2, apparatus camera view and layout of County HWY 5 & Louisiana Ave S.

Site 3, the intersection of Snelling Ave. and County Road B, consists of a Southbound 5 lane approach with two isolated lefts and right (5-lanes, A), plus a 4-lane Northbound approach with near-side isolated right turn (4-lanes-B). This site was used to run experiments to extract isolated right turn traffic flows as well as the other mainline lane flows on upwards of 4 and 5 lanes. The circled right turn movements at the top of the video image had the largest count errors. This was also predicted by the occlusion analysis. The system was deployed at this site for a total of 106 hours. The weather conditions during the deployment period varied from sunny to heavy rain and thunderstorms with a maximum wind speed of 43 mph.

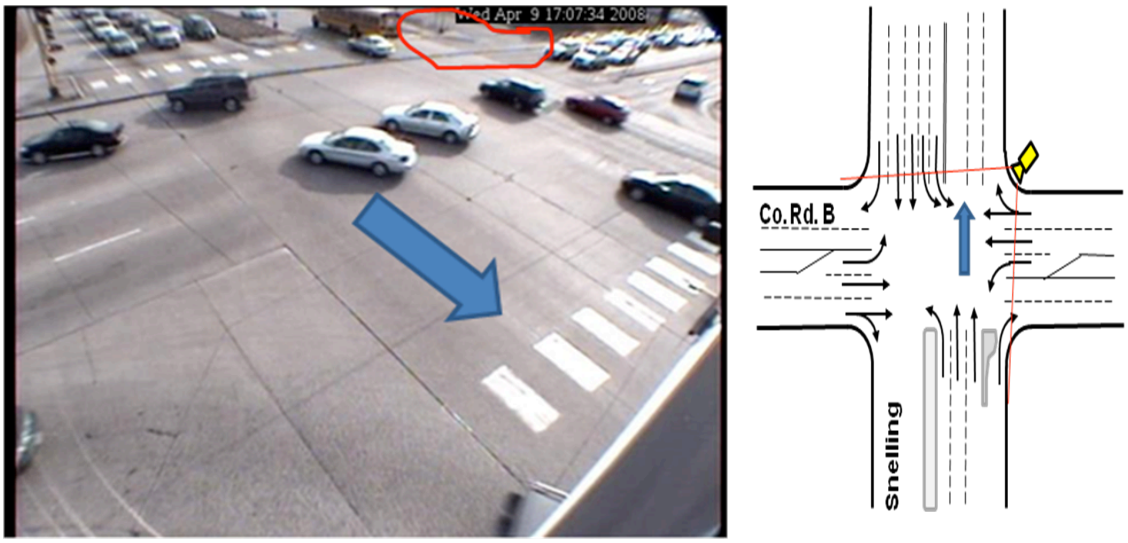

Figure 8: Site 3, apparatus camera view and layout of Minnesota State Highway 51 (Snelling Ave.) and County Road B.

The circled right turn movements in Figure 6 at the top of the video image had the largest count errors. This was also predicted by the occlusion analysis.

Site 4, Highway 252 and 66th Ave North, the largest intersection lane geometry configuration for the urban arterial candidates being considered here, consists of a North bound 6-lane approach with two exclusive left turn lanes and one exclusive right (6 lanes-A). The circled approaches in the geometry schematic in Figure 8 could not be counted with the single camera set up. The occlusion analysis predicted that the other possible set up location for this sight on the south east corner of the intersection contained significant cross lane occlusion errors. Looking at the above figure it is obvious that occlusion is going to be concern. For the configuration deployed as illustrated in Figure 8, the camera height and field of view was not able to adequately capture the NE or WS right

movements. The system was deployed at this site for a total of 106 hours. The weather conditions during the deployment period varied from sunny to heavy fog with a

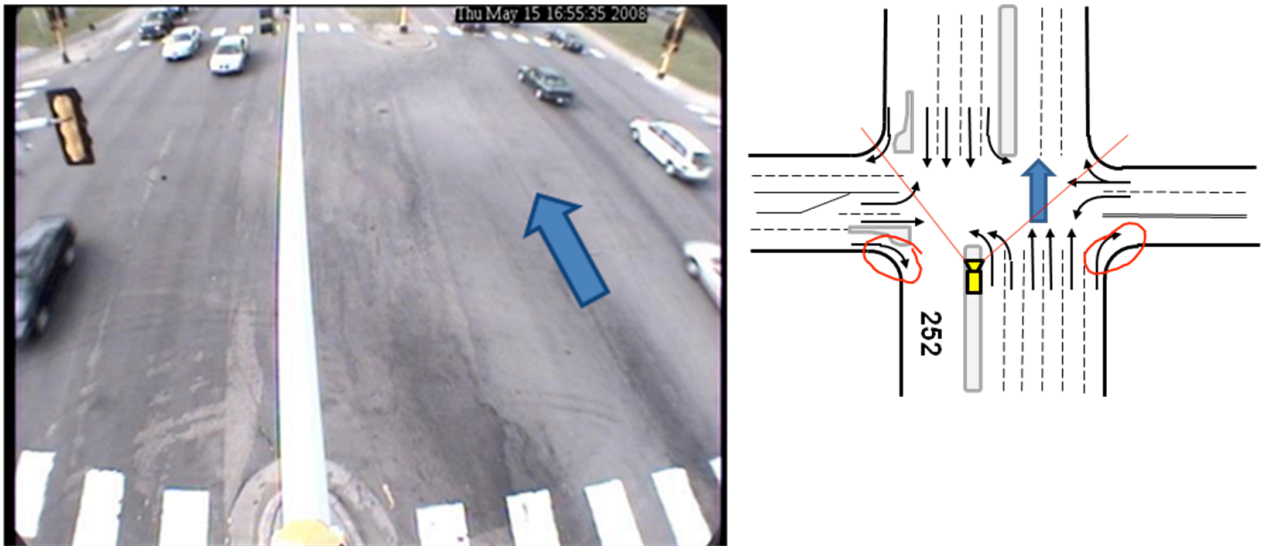

maximum wind speed of 17 mph.

Figure 9: Site 4, apparatus camera view and layout of Minnesota State Highway 252 and 66th Ave. North.

Site 5, SE University Ave. near SE 16th Ave., is the location utilized for mid-block detection. It consists of only a eastbound 3-lane one-way arterial approximately 250 feet before a signalized intersection (3 lanes-B). The system was deployed at this site for a total of 5 hours. The weather conditions during the deployment period varied from sunny to overcast with a maximum wind speed of 13 mph.

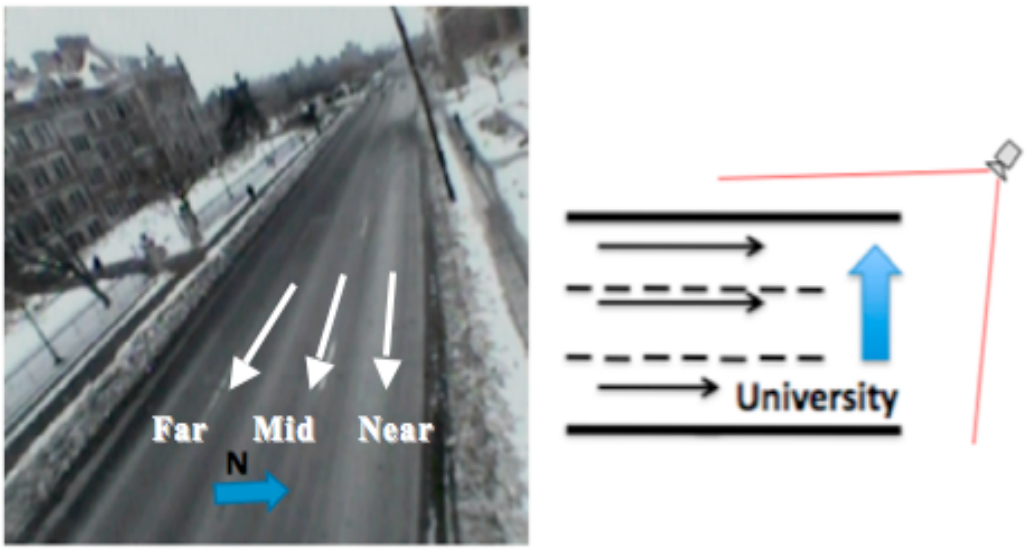

Figure 10: Site 5, apparatus camera view and layout of SE University Avenue and SE 17th Ave.

Site 6, Olsen Memorial Highway and Glenwood Ave, is the location utilized for queue length detection. It consists of a Northbound and Southbound 2 X 3-lane highway approach (3 lanes-B). The system was deployed at this site for two full weeks. The weather conditions during the deployment period varied from sunny to overcast with a maximum wind speed of 19 mph.

Figure 11: Site 6, apparatus camera view and layout of Olsen Memorial HWY and Glenwood Ave.

F. Ground Truth Process

In order to analyze the collected data a ground truth process was carried out. The resulting measurement errors between the ground truth and the automated extracted data were then analyzed using several statistics. The ground truth procedures for each traffic measurement are described below.

Volume

Each test requires a ground truth by which the test results can be compared. For turning a volume counts a visual ground truth of the video files was carried out using a JAMAR Technologies Inc. manual counting box. After each set of video files were manually ground truthed, a random subset of those files underwent a second round of visual ground truthing which was then compared to the first set to ensure the data was accurate. When errors were found the entire set underwent a second round of ground truthing to ensure the error was negligible. Such a ground truth process is far less prone to error as the video files can be stopped at the end of any data interval and the video could then be rewound to isolate known error or for any instance where the counter needed a break. Such manual counts were then imported into Microsoft excel where they were compared to the test data. For all volume counts analyzed herein, volume counts were aggregated and tabulated every 15 minutes (thus the data intervals were always 15 minutes).

The variability between the ground truth and the extracted volume counts were analyzed using the R^2 correlation coefficient and Pearson's R. Under or over counting trends were examined using the Mean Percent Error (MPE) relative to the ground truth measurements. Overall counting accuracy was quantified using the Mean Absolute Percent Error (MAPE). The error proportions for both the MPE and MAPE are relative to the ground truth 15-minute approach count value.

Vehicle Speed and Classification

For mid-block testing the ground truth required a series of methods. For classification, prior to any testing, the collected video was viewed and the vehicle classification ground truth was collected manually. As stated above, the volume was ground truthed manually using a JAMAR Technologies Inc. manual counting box. Lastly, the vehicle speed was ground truthed manually by setting markers on the video at set distances and then calculating the number of frames it took each vehicle to travel from the upstream marker to the downstream marker. The following equation was used to estimate vehicle space mean speed in miles per hour, denoted S_{mph}.

(1)

$$S_{mph} = \left(\frac{d_m \times f_s}{t_{us} - t_{ds}}\right) \times \frac{3600\ sec}{hr} \times \frac{1\ mile}{5280\ ft}$$

Where d_m is the distance between markers, f_s is the video file frame rate (frames per second), t_{us} and t_{ds} are the times at which the vehicle crossed the upstream and downstream marker respectively.

The variability between the ground truth and the extracted mean speeds were analyzed using the R^2 correlation coefficient and Pearson's R. Under or over estimates in speed were examined using the Mean Percent Error (MPE) relative to the ground truth measurements. Overall counting accuracy was quantified using the Mean Absolute Percent Error (MAPE). Three classification levels (private vehicles, recreation vehicles, and heavy vehicles) were used for this experiment. Including the initialization interval, 2 hours and 15 minutes of video were analyzed for this experiment.

G. Statistical Methodology

In this thesis there are five statistical measures utilized. These measures include; the variance, the coefficient of determination (R-Squared), the correlation coefficient, the mean percent error and the mean absolute percent error.

Note: Due to the extreme errors seen in the tracking feasibility study, it was determined that detailed statistical analysis was not necessary.

Variance

The first statistical measure is the variance. If random variable X has expected value (mean) $\mu = E(X)$, then the variance Var(X) of X is given by:

(4)

$$Var(X) = E\left[(X - \mu)^2\right]$$

In our case; since the random variable X is discrete

(5)

$$Var(X) = \sum_{i=1}^{n} \rho_i \left[(x_i - \mu)^2\right]$$

Where the probability mass function $x_1 \rightarrow p_1, x_2 \rightarrow p_2, ..., x_n \rightarrow p_n$.

It is therefore the average of the square of the distance of each data point from the mean [23]. The value of the variance is between 0 and 1, where the closer the value is to 1 the closer the machine-measured values are to the ground truthed values.

Pearson Product-Moment Correlation Coefficient

Correlation indicates the strength and direction of a linear relationship between two

random variables. The coefficient of a correlation measures the degree of such a correlation. The Pearson product-moment correlation coefficient is obtained by dividing the covariance of the two variables by the product of their standard deviations (equation 5).

The coefficient ranges from −1 to 1. A value of 1 shows that a linear equation describes the relationship perfectly and positively, with all data points lying on the same line and with Y increasing with X. A score of −1 shows that all data points lie on a single line but that Y increases as X decreases. A value of 0 shows that a linear model is not needed – that there is no linear relationship between the variables [24].

The statistic is defined as the sum of the products of the standard scores of the two measures divided by the degrees of freedom [24]. Given the data comes from a sample rather than a population, as it does in this thesis:

(6)

$$r = \frac{1}{n-1}\sum_{i=1}^{n}\left(\frac{X_i - \overline{X}}{s_X}\right) * \left(\frac{Y_i - \overline{Y}}{s_Y}\right)$$

Where s_X is the sample standard deviation (calculated using n − 1 in the denominator), $\overline{X}$ is the sample mean, and thus $\left(\frac{X_i - \overline{X}}{s_X}\right)$ is the standard score [24].

Linear regression describes the relationship between the X and Y values, whereby the correlation coefficient is used in predicting the value of the actual count from knowledge of the measured value. That is, for each value of X the equation calculates a value, which is the best estimate of the values of Y corresponding the specific value [24].

Coefficient of Determination

The next statistical measure is the coefficient of determination. The coefficient of determination is denoted as R-Squared R^2. This value provides a measure of how well future outcomes are likely to be predicted by the model [25]. R^2 is the square of the

sample correlation coefficient between the outcomes and their predicted values; in our case, between the machine-measured and ground truthed values.

A data set has values y_i each of which has an associated modeled value f_i. Here, the values y_i are the machine-measured values and the f_i values are the ground truthed values. The "variability" of the data set is measured through different sums of squares. The R^2 value is equal to one minus the error in the sum of squares (proportional to the variance) divided by the total sum of squares denoted:

(7)

$$R^2 = 1 - \frac{\sum_i (y_i - f_i)^2}{\sum_i (y_i - \bar{y})^2}$$

Where $\bar{y}$ is the mean of the modeled data and (i) represents each individual sample.

The resulting R^2 value is between 0 and 1, where the closer the value is to one, the more likely the future outcomes are likely to be predicted by the model, thus well correlated.

The square of the Pearson correlation coefficient is traditionally used as a measure of the association between X and Y. This means that if R^2 is 0.90, then 90% of the variance of Y can be "accounted for" by changes in X and the linear relationship between X and Y [24].

Mean Percent Error

Mean percent error (MPE) measures the accuracy in a fitted time series value in statistics. Oftentimes this is used in trending. The MPE commonly is used for expressing accuracy as a percentage, however, differs from many trend statistics in that it looks for the overall aggregate error rather than the sum of each individual value error. It has application in this thesis regarding total volumes, as each individual interval error is less important to practitioners than the aggregate value over an extended length of time. In mathematical terms, MPE is defined as:

(8)

$$MPE = \frac{1}{n}\sum_{i=1}^{n}\left[\frac{A_t - F_t}{A_t}\right]$$

Where n is the sample size, A_t is the actual value which is the ground truth count, and F_t which is the forecasted value, the machine-measured value herein.

Mean Absolute Percent Error

The Mean Absolute percent error (MAPE) is very similar to the MPE discussed above in that it measures the accuracy in a fitted time series value in statistics. The MAPE is used for expressing the accuracy as a percentage of the sum of each individual value error. The MAPE allows us to visualize a system's error as compared to a ground truth in order to determine the true drawbacks of the system. When the MAPE is compared to the MPE, we can see the difference between the system utility versus the data utility. The MAPE is calculated as follows:

(9)

$$MAPE = \frac{1}{n}\sum_{i=1}^{n}\left|\frac{A_t - F_t}{A_t}\right|$$

Where again, the n is the sample size, A_t is the actual value which is the ground truth in this thesis, and F_t which is the forecasted value, in this thesis the machine-measured value.

H. Data And Occlusion Analysis Methodology

Ground truth data was obtained manually using a JAMAR counting device from the 106 hours of video recordings. Tabulated every 15 minutes, the manual counts were tested for accuracy by randomly selecting three hours of recording to have another person extract the same information. Subsequently the two data sets were compared to test the manual accuracy. The comparison yielded counting errors of less than one percent.

Video from Site 3 at Snelling Ave. and CTY Rd B, (Figure 24) and Site 4 at HWY 252 and 66th St., (Figure 27) required multiple passes in order to carry out manual ground truthing. The extreme number of lanes per approach at these intersections in conjunction with the high volumes of vehicles passing through these intersections during peak periods made manual counting difficult. Though counting of half the intersection at each pass, the data collected were ensured to be accurate and was later checked for accuracy through the method stated above.

Several studies were consulted [26], [27] for understanding the affects of camera placement on traffic measurement errors extracted from video image sequences. Specifically, these studies [26], [27] focus on predicting and analyzing the affects of occlusion between 'overlapping' vehicles. For example, TTI [27] utilized mathematical models and concluded that occlusion comes into play immediately beyond the first lane and thus is a major issue. Other studies developed analytical techniques based on modeling most vehicle classes, the road or intersection geometries, camera placement, and optics [27]. Occlusion analysis for camera aspects pointing laterally across lanes as well as pointing longitudinally down the lane was developed [26]. We utilized the analytical method formulated by [26] which was based on dense vehicular traffic even at safe space headways. Camera height, lateral offset position from the roadway, and camera angle were varied in order to determine their individual or combined affects on background and total occlusion errors. Background occlusion occurs when vehicles are too closely spaced together for the video to see any spacing between them. Total occlusion exists when a larger vehicle inhibits any view of a smaller vehicle behind it.

All occlusion findings are based on the use of CCD analog cameras (used in practice) in regular viewing mode.

Mathematical Analysis

The following mathematical model was implemented through excel to better understand what vehicle occlusion would be encountered during deployment. In order to create such a model the following assumptions were made.

Assumptions:

- The monitoring point and thus each vehicle is assumed to be in the center of the lane
- All cars are assumed to have a constant height of 5 feet and a length of 18 feet.
- All trucks are assumed to have a constant height of 15 feet and a length of 40 feet.
- For cross-lane occlusion analysis all vehicles are assumed to be elliptical cylinders with major axis (dy) as the vehicle length and minor axis (dx) as the vehicle width.
- For down-lane occlusion analysis all vehicles are assumed to be rectangular cubes of length $dy1, dy2$, width $dx1, dx2$ and height $h1, h2$ for lead and trail vehicles respectively.
- All roadway lanes are of equal width (12 feet)

Variables:

- The height of the lead and trail vehicles is denoted $h1, h2$ respectively
- The space headway is denoted s.
- The lead and trail vehicle diameter is denoted $d1, d2$ respectively.
- The distance from the lead vehicle to the roadway viewing point (pole base) is denoted b.

- Vehicles are separated by N lanes where $(N > 0)$.

We will first examine occlusion when viewing a vehicle straight down a lane. This will help in generalizing the occlusion conditions to any position on the roadway.

The geometry used for this analysis is shown in Figure 12. A point on the road is being viewed from a camera on a pole of height h at a distance d from the base of the pole. We will look at two types of occlusion limits: background and total vehicle.

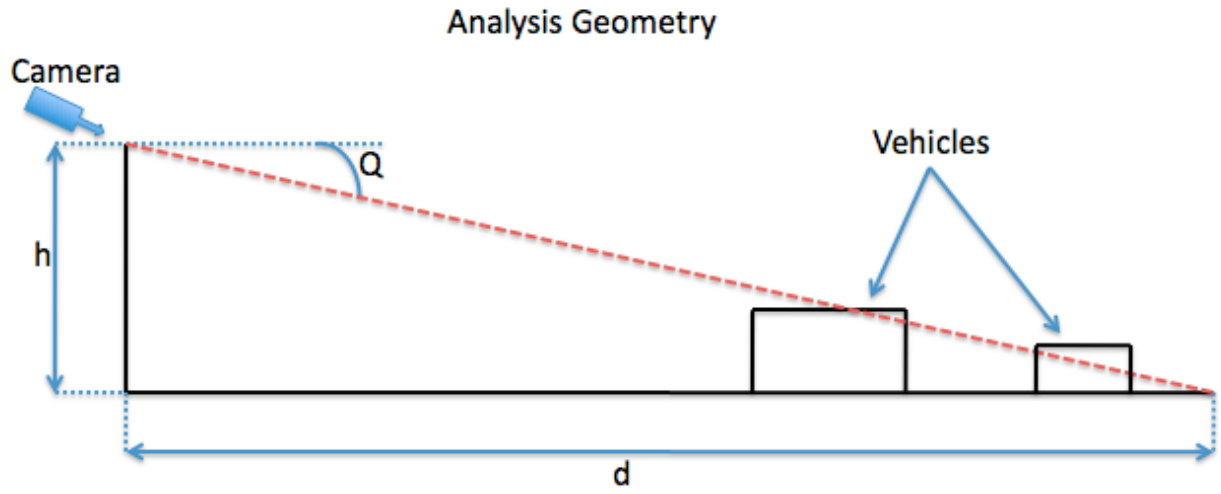

Figure 12: Geometry of vehicle occlusion model. The vehicle on the left is a larger vehicle (like a truck) while the vehicle on the right is smaller vehicle (more like a car).

Background Occlusion:

The geometry for analyzing background occlusion is shown in Figure 13. The height of the first vehicle is $h1$ and the spacing between vehicles is s. Background occlusion occurs when:

$$z < h1$$

Such that $z = s \times \tan(Q)$. Since $\tan(Q) = h/d$, occlusion occurs when:

[a]

$$s \times (h/d) < h1$$

For a pole height of 40 feet at a distance of 200 feet, $(h/d) = 1/5$.

Therefore, background occlusion can be expected for any **car space headway of less than 25 feet** or **truck space headway of less than 75 feet**.

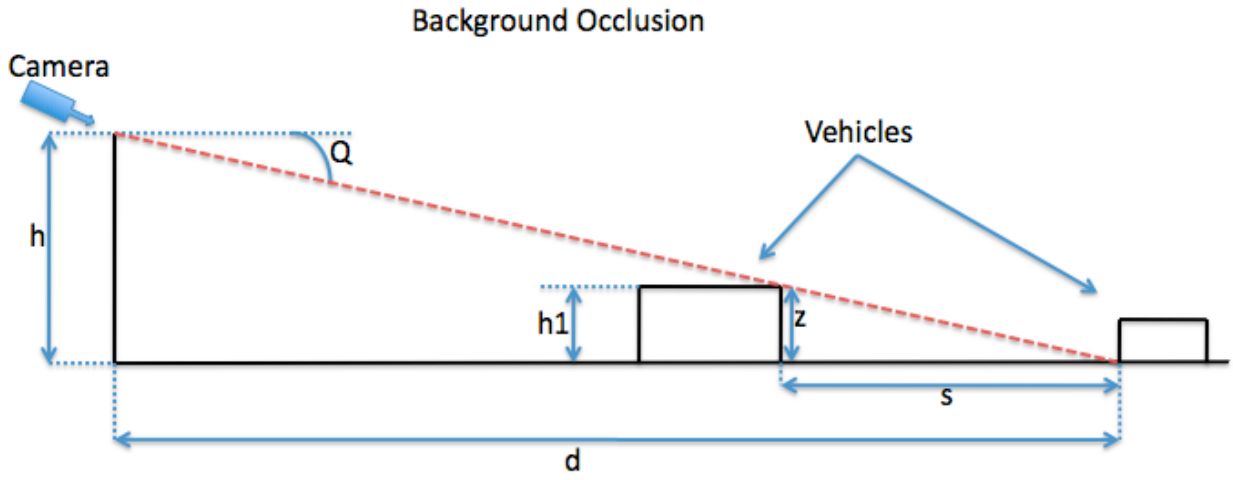

Figure 13: Geometry of background occlusion.

Total Occlusion:

The geometry for analyzing total occlusion is shown in Figure 14 below. The height of the leading vehicle is $h1$ and the height of the trailing vehicle is $h2$, the diameter of the trailing vehicle is $d2$, the spacing between vehicles is s and the distance between the leading vehicle and the roadway viewing point is b. Total occlusion of the trailing vehicle occurs when:

[b]

$$h2 < [h1 - (s + d2) \times \tan(Q)]$$

The above equation is derived by finding the distance the leading vehicle is from the roadway viewing point when occlusion ends. This is:

[c]

$$b = h1/\tan(Q)$$

Then from this, the above limit is found by:

[d]

$$h2 < [b - (s + d2)]\tan(Q)$$

By [c] and [d], we derive [b]. Again $\tan(Q)$ is the ratio h/d so equation [b] can be represented as:

[e]

$$h2 < [h1 - (s + d2)(h/d)]$$

Conversely,

[f]

$$h1 > [h2 + (s + d2)(h/d)]$$

What is really of interest is the relation relative to differences in vehicle heights, so the relation can be rewritten as:

[g]

$$(h1 - h2) > (s + d2)(h/d)$$

When the leading vehicle is a truck $(h1 = 15\,feet)$, total occlusion occurs for $s < 35\,feet$ when $h/d = 1/5$. When both vehicles are cars $(h1 = h2)$ then total occlusion never occurs.

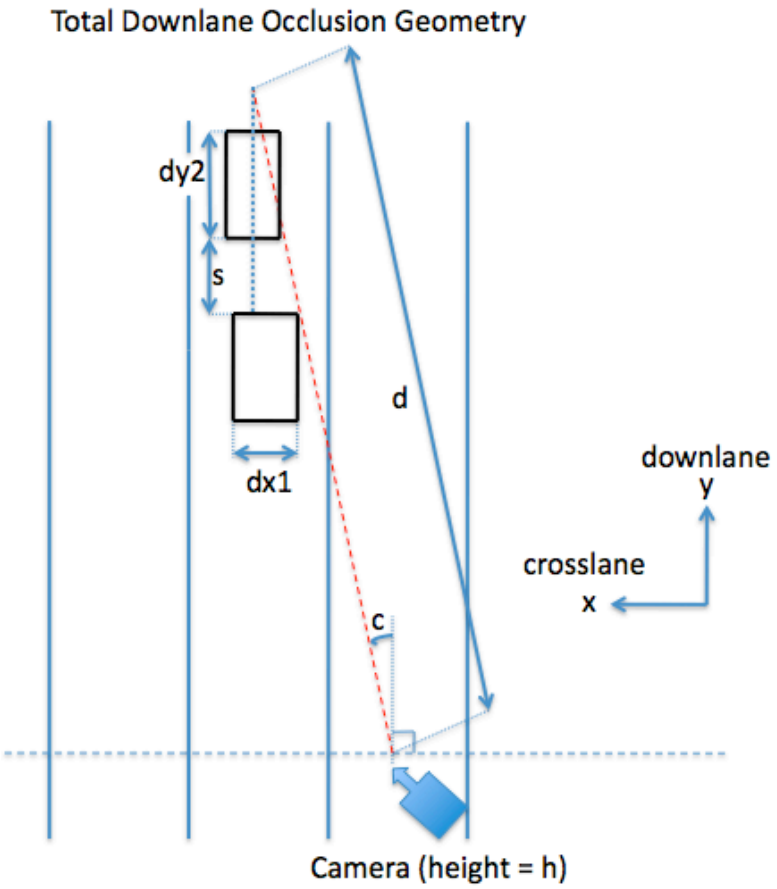

Figure 14: Geometry of total downlane occlusion model.

Cross-lane Occlusion:

The geometry for analyzing crosslane occlusion is shown in Figure 15. We assume that vehicles are elliptical cylinders with major axis (dy) as the vehicle length and the minor axis (dx) as the vehicle width. Therefore, the previous relations will apply at any road position if the vehicle separation s and the vehicle diameter d1 or d2 are properly computed. We will assume that the vehicles are separated by N lanes (N>0).

For this model, we will assume that the ellipse centers line up on the line of sight of the camera. To use the occlusion limit equations above, s and d2 must be computed based on

the angle with respect to the crosslane axis (angle C) and the two vehicle sizes (represented by dx1, dy1 and dx2, dy2 diameters). To compute s and $d2$ we derive them from the following:

[h]

$$s = [NL/[|\sin(C)|] - [(d2 + d1)/2]$$

And then,

$$d1 = \sqrt{[(dx1)\sin(C)]^2 + [(dy1)\cos(C)]^2}$$

Therefore,

[i]

$$d2 = \sqrt{[(dx2)\sin(C)]^2 + [(dy2)\cos(C)]^2}$$

Using the above relations, equations [a] and [g] can be used directly for cross-lane background and total occlusion:

[j, k respectively]

$$s(h/d) < h1$$

$$(h1 - h2) > (s + d2)(h/d)$$

This is sensitive to the number of lanes and not to the type of vehicle.

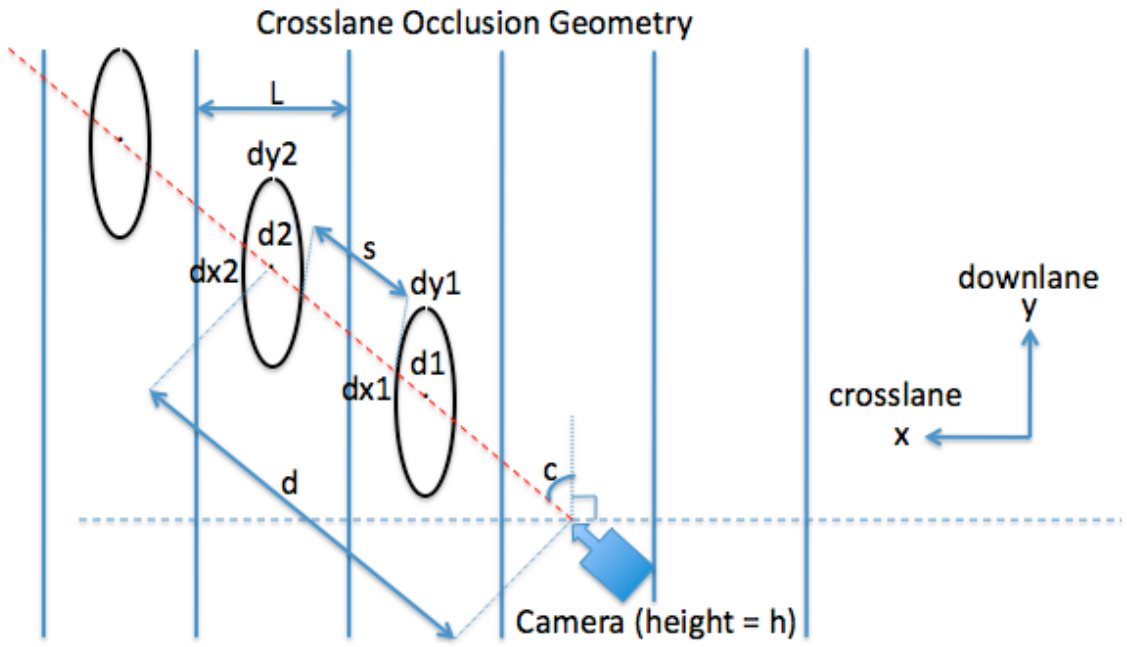

Figure 15: Geometry of crosslane occlusion model.

Down-lane Occlusion:

For downlane occlusion we assume rectangular vehicles of width $dx1$, $dx2$, length $dy1$, $dy2$ and height $h1$, $h2$ and centered in the middle of lanes. The analysis geometry is show in Figure 16 below.

There are two relations for background occlusion, one due to the height (e.g. equation [a]) and another due to the vehicle width. The height is the only relation for straight downlane viewing angles (i.e. $c = 0$ degrees), but for any other angle, both the width and height are factors. The choice of which relation to use is a function of the following expressions:

$$z1 = h1/\tan(Q)$$
$$z2 = (dx1/2)/\sin(C)$$

Where the back of vehicle one intersects the line of sight in the vertical direction is $z1$ (like in equation [a]). Where the side of vehicle one intersects the line of sight in the crosslane direction is $z2$.

If $z1 < z2$ then only the vehicle height determines the occlusion limits since the viewing point can be seen for any larger vehicle spacing s regardless of the vehicle width. But if $z1 > z2$ then the vehicle height occludes only up to the car spacing of $z2$ and then the view point can be seen around the first vehicle regardless of the vehicle height.

So, the following background occlusion relation exists:

[l]

$$s/\cos(C) < MIN[h1/\tan(Q),(dx1/2)/\sin(C)]$$

The $\cos(C)$ term results in s being the downlane car spacing instead of the diagonal spacing. This results in the downlane background occlusion limits being:

[m]

$$s < MIN[h1(\cos(C))/\tan(Q),(dx1/2)/\tan(C)]$$

For total occlusion, the geometry in Figure 16 below is used. For total occlusion there are relations similar to those from background occlusion, but the b term in equation [d] has two possible values:

[n, o respectively]

$$b1 = h1/\tan(Q)$$
$$b2 = (dx1/2)/\sin(C)$$

If $b1 < b2$ then the first height term determines the total occlusion limits, otherwise the second term is used.

[p]

$$b = MIN[b1,b2]$$

The equation in equation [n] can be directly substituted in equation [d] with the $(s + dy2)$ term divided by $\cos(C)$.

$$h2 < [b - (s + dy2)/\cos(C)]\tan(Q)$$

This can be re-written as:

$$s < [b - (h2/\tan(Q))]\cos(C) - dy2$$

Note that if $b = b1$ and $c = 0$, this is the same as equation [g].

Substituting equation [p] for b, and h/d for $\tan(Q)$, the condition for downlane total occlusion at any viewing angle C is:

[q]

$$s < [MIN[b1,b2] - h2(d/h)]\cos(C) - dy2$$

Where $b1 = h1/\tan(Q)$ and $b2 = (dx1/2)/\sin(C)$.

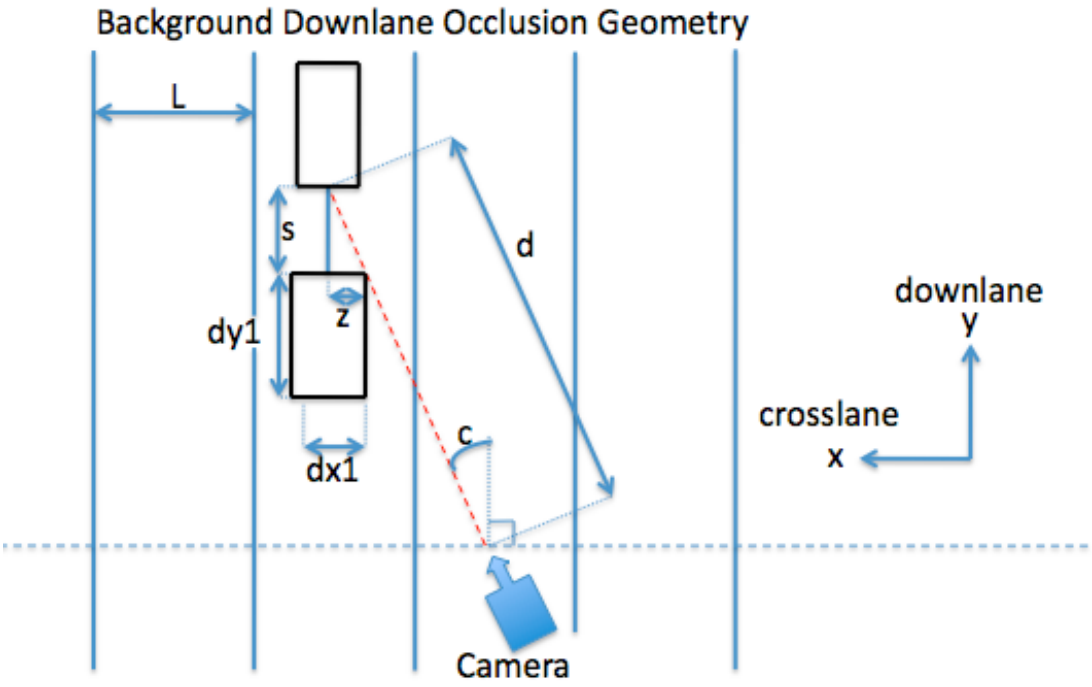

Figure 16: Geometry of background occlusion model.

From the above mathematical equations a mathematical graph could be constructed to help visualize the threshold at which occlusion becomes an issue given a camera height of 35 feet.

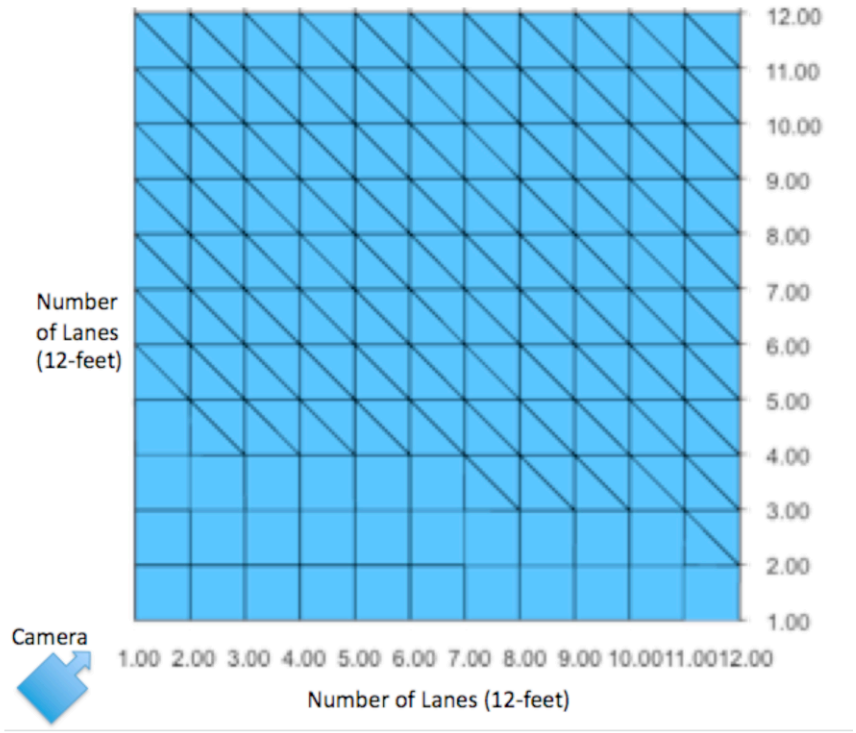

Figure 17: Graphical occlusion potential (per lane) from camera.

As stated above, the above graph (Figure 17) is used to understand the threshold in which any form of occlusion can be expected. It assumes the camera is of standard offset from the intersection (roughly 12 feet) and 35 feet high at what would be (0,0). The image shows cross hashes where occlusion can exist given standard headways, thus at lane two horizontal and two vertical from the camera, there is no real potential for occlusion but at three across and two vertical there is potential for occlusion. Using this as a road map against the layout of the intersections, we can determine where occlusion will likely exist. Given the above analysis, occlusion is not avoidable as all test intersections contain some amount of occlusion and thus require visible analysis to determine the intensity of the potential occlusion. Based on the aforementioned analytical models and visual observations, we determined the occlusion affects at all sites, which are as follows:

Site 1: No total occlusion exists; however, background occlusion occurs if and only if a through moving truck on the down lane approach coincides with a car making a right turn on the far approach (the approach farthest from the camera). This occlusion is unlikely to

cause problems, as there is ample time for the video-processing algorithm to differentiate the two vehicles. The minimum height for the video camera to be placed for best results is at least 30 feet. This should prevent total occlusion and minimize background occlusion based on the mathematical occlusion modeling.

Figure 18: Site 1 – Occlusion analysis – no notable occlusion exists.

The above figure (Figure 18), visually confirms that occlusion while may exist, is not of major concern. The eastbound and westbound vehicles seen in the above figure visual demonstrate that the image background (street) is visible despite both a trailing vehicle and a vehicle in a neighboring lane.

Site 2: Total Cross lane occlusion exists anywhere but the closest lane to the camera as shown at the top right image of Figure 19. Based on the mathematical occlusion data, the far down lane is highly susceptible to total occlusion in certain areas of movement. The

empirical data from videos already collected show a larger intersection with similar points of interest regarding occlusion, meaning such occlusion can exist. In a larger intersection that resembles Site 4, total occlusion exists on a limited basis and not for the duration of vehicular movement through the entirety of the intersection, whereas, at this site it will depend on the percentage of large vehicles seen in the video and which lanes these large vehicles occupy.

Figure 19: Site 2 - Occlusion analysis, trucks can create total occlusion.

Figure 20: Site 2 - Occlusion analysis, cars create no notable occlusion.

Site 3: Total down lane and cross lane occlusion exists in the farthest (from the camera) three lanes. Cross lane occlusion seems to suggest more of a problem due to constant similarities between adjacent vehicles thus making two vehicles appear to be one. Color differentiation may not be enough in this case if partial occlusion gives way to total occlusion during vehicle travel through the intersection. It is likely that two camera setups will be needed for more accurate counting.

Figure 21: Site 3 - Occlusion analysis, cars create only background occlusion.

Site 4: The occlusion is very similar to Site 3 except that the separated turning counts if they can be captured on the video will be very accurate, from the image it appears that only two of the turning movements will be visible thus only they can be counted. There is no occlusion on the separated right turns of which only one if the top left corner of the image can be seen, however the multiple through lanes unless directly next to the camera mount all have partial occlusion. The far lane on each direction can have total occlusion if semi-tracker trailers are present. Two cameras will most likely be needed here, however, a second system was not available for testing.

The "peak hour factor" or PFH, was used in the occlusion study to estimate the magnitude of occlusion error, as speeds are more uniform when this factor increases the probability of error prone areas are more in parallel. This increase has not been considered in previous studies and could pose additional questions for future

consideration such as the possible use of infrared cameras. As the PHF increases density increases, therefore causing "downlane" occlusion to increase substantially; however, upon deployment it was found that because of the camera placement selections such occlusion issues were minimal and they did not play a significant role in the data accuracy. For example, there were consistently areas in which occlusion did not persist unless semi-tractor trailers were involved which made up less than 5 percent volumes typical at urban test sites.

Figure 22: Site 4 - Occlusion analysis, cars create no notable occlusion.

The above figure (Figure 22) demonstrates the utility of placing the camera at the median of the intersection such that the distance of each lane from the camera in minimized and limits the potential for occlusion.

I. Data Collection and Testing

As mentioned previously in the thesis, before the first prototype was built, a modified system was deployed to further understand deployment issues and practical camera configurations. In addition, the collected data were also used to test the feasibility of an available machine vision tracking algorithm to separate turning and thru movements from three intersections. The advantage of using the tracking algorithm is that approach counts and turning counts are automatically extracted with minimal set-up time. The basis of the algorithm is extracting and tracking blob representations of foreground vehicles from the background scene [12,13]. The research team developed efficient camera calibration procedure as part of the tracking algorithm, which inherently defined thru and turning movements for tracked vehicles in the intersection [13].

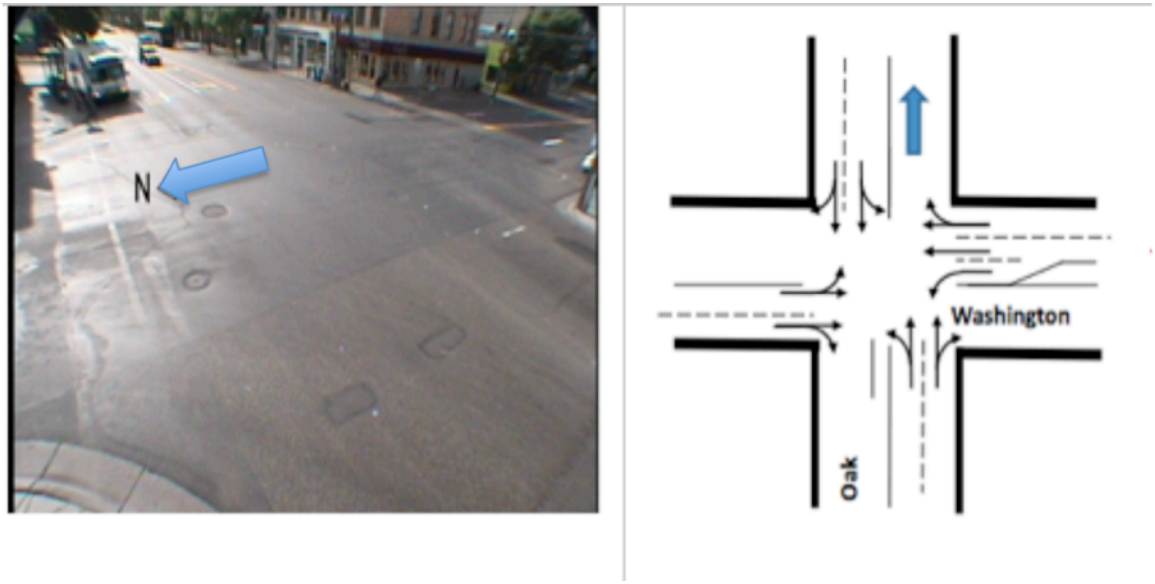

Figure 23: Tracking Site B: Oak Street & Washington Ave. Note the mixed left/thru for the North and South bound approaches.

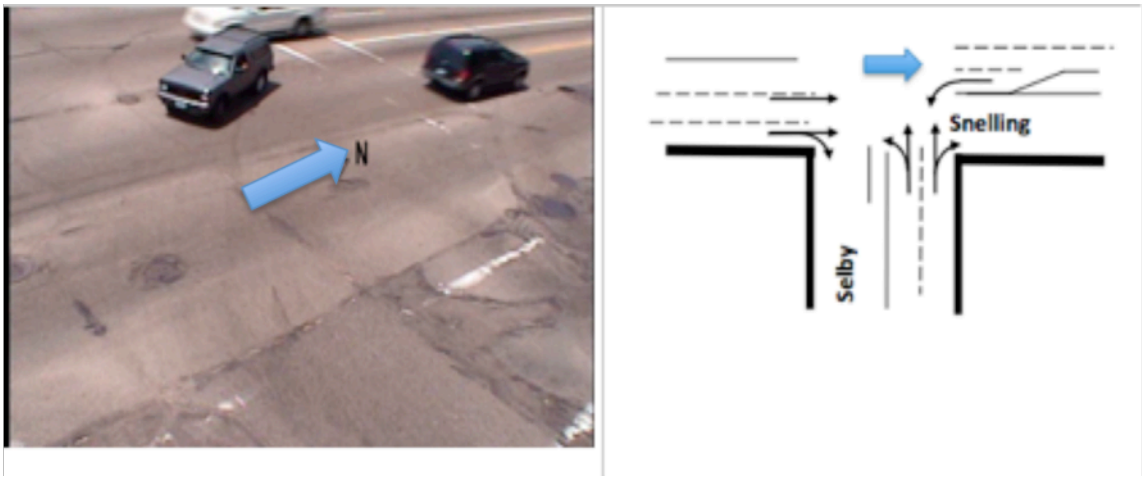

Figure 24: Tracking Site C: Half of the intersection of Selby Street and Snelling Ave..

Only half the intersection was recorded in order to test the affects this might have on tracking accuracy and the test results show similar error to other sites. Three separate one-hour video recordings from each of three intersection sites were examined. The three intersections were comparable in size and number of lanes per approach to intersections in the aforementioned intersection field data collection sites (Figures 23-25). Under all circumstances, significant counting errors resulted for many of the vehicle movements. Variability in counting errors was not attributed to levels of traffic volume, cross lane or down lane occlusion, or intersection geometry. Note that uncompressed digital video as well as MPEG4 video with similar bit rate and quality settings used with the current prototype were also tested with no consistent patterns of measurement errors observed. Tables 5 - 7 summarize the results.

Table 5: University Ave. and Snelling Ave. (Tracking Site A) results.

University and Snelling														
Ground Truth														
Start Time	Duration	Total	S-N	N-S	W-E	E-W	W-N	W-S	E-N	E-S	S-W	S-E	N-W	N-E
10:00:00 AM	15	631	180	104	67	77	12	32	30	29	29	32	13	26
10:15:00 AM	15	612	154	93	56	84	13	46	23	29	41	32	18	23
10:30:00 AM	15	710	180	122	61	104	12	30	35	39	44	36	19	28
10:45:00 AM	15	700	183	122	81	90	14	38	25	35	39	40	9	24
Totals	**60**	**2653**	**697**	**441**	**265**	**355**	**51**	**146**	**113**	**132**	**153**	**140**	**59**	**101**
Extracted														
Start Time	Duration	Total	S-N	N-S	W-E	E-W	W-N	W-S	E-N	E-S	S-W	S-E	N-W	N-E
10:00:00 AM	15	1010	179	278	195	200	20	31	16	26	27	27	1	10
10:15:00 AM	15	1007	178	277	174	218	28	28	14	30	27	15	3	15
10:30:00 AM	15	1155	201	345	206	208	32	37	15	27	34	24	4	22
10:45:00 AM	15	1180	222	392	206	187	31	34	11	32	34	18	3	10
Total	**60**	**4352**	**780**	**1292**	**781**	**813**	**111**	**130**	**56**	**115**	**122**	**84**	**11**	**57**
Hourly % Accuracy		**61**	**89**	**34.13**	**34**	**44**	**46**	**89**	**50**	**87**	**80**	**60**	**19**	**56**
Total Miscounts		**1699**	**85**	**851**	**516**	**458**	**60**	**30**	**57**	**19**	**31**	**56**	**48**	**44**
Average % Accuracy		**57.3**	**%**											
Miscount Total		**2255**	**of**	**2653**	**actual vehicles**				**=**	**85**	**%**			

Table 6: Tracking Site B: Oak St. and Washington Ave. results.

Oak and Washington														
Ground Truth														
Start Time	Duration	Total	W-E	E-W	N-S	S-N	N-E	N-W	S-E	S-W	W-N	W-S	E-N	E-S
10:00:00 AM	15	323	53	106	42	11	5	26	9	5	29	13	3	21
10:15:00 AM	15	302	61	103	40	9	4	17	5	10	19	12	4	18
10:30:00 AM	15	267	57	81	32	6	2	20	10	8	13	21	5	12
10:45:00 AM	15	256	49	74	27	15	2	16	12	3	19	13	5	21
Total	**60**	**1148**	**220**	**364**	**141**	**41**	**13**	**79**	**36**	**26**	**80**	**59**	**17**	**72**
Extracted														
Start Time	Duration	Total	W-E	E-W	N-S	S-N	N-E	N-W	S-E	S-W	W-N	W-S	E-N	E-S
10:00:00 AM	15	628	159	144	65	53	2	13	37	11	69	25	32	18
10:15:00 AM	15	540	125	164	48	44	4	11	32	14	46	15	26	11
10:30:00 AM	15	490	102	133	52	42	5	10	33	18	50	23	13	9
10:45:00 AM	15	434	130	103	35	17	8	8	28	11	51	13	19	11
Total	**60**	**2092**	**516**	**544**	**200**	**156**	**19**	**42**	**130**	**54**	**216**	**76**	**90**	**49**
Hourly % Accuracy		**54.9**	**42.6**	**66.9**	**71**	**26**	**68**	**53**	**28**	**48**	**37**	**78**	**19**	**68**
Total Miscounts		**944**	**296**	**180**	**59**	**115**	**12**	**37**	**94**	**28**	**136**	**17**	**73**	**23**
Average % Accuracy		**50.4**	%											
Miscount Total		**1070**	of	**1148**	actual vehicles				=	**93**	%			

Table 7: Tracking Site C: Half of the intersection of Selby St. and Snelling Ave. results.

Snelling and Selby														
Ground Truth														
Start Time	Duration	Total	S-N	N-S	W-E	E-W	W-N	W-S	E-N	E-S	S-W	S-E	N-W	N-E
10:00:00 AM	15	438	184	97	20	26	10	0	40	7	7	6	0	41
10:15:00 AM	15	396	147	80	23	27	11	0	43	10	4	2	0	49
10:30:00 AM	15	404	174	73	29	19	7	0	43	6	4	6	0	43
10:45:00 AM	15	410	174	80	26	15	7	0	41	6	4	6	0	51
Totals	**60**	**1648**	**679**	**330**	**98**	**87**	**35**	**0**	**167**	**29**	**19**	**20**	**0**	**184**
Extracted														
Start Time	Duration	Total	S-N	N-S	W-E	E-W	W-N	W-S	E-N	E-S	S-W	S-E	N-W	N-E
10:00:00 AM	15	536	217	87	84	84	3	10	1	21	3	19	0	7
10:15:00 AM	15	572	209	116	90	76	3	3	1	20	14	28	0	12
10:30:00 AM	15	549	201	125	73	80	4	7	0	13	9	26	0	11
10:45:00 AM	15	516	181	94	84	88	2	4	1	20	7	24	1	10
Total	**60**	**2173**	**808**	**422**	**331**	**328**	**12**	**24**	**3**	**74**	**33**	**97**	**1**	**40**
Hourly % Accuracy		**75.8**	**84**	**78.2**	**30**	**27**	**292**	**0**	**1.8**	**39**	**58**	**21**	**0**	**22**
Total Miscounts		**525**	**129**	**112**	**233**	**241**	**23**	**24**	**164**	**45**	**22**	**77**	**1**	**144**
Average % Accuracy		**54.2**	**%**											
Miscount Total		**1215**	**of**	**1648**	**actual vehicles**				**=**	**74**	**%**			

Based on the above results, it is the recommendation of this study to avoid using the above tracking algorithm in respect to the apparatus and site experiments completed herein. Previous studies by Tarko and Lyles (2002) demonstrated that volume counts with simple 'tripwire' presence detectors utilizing a commercially and widely available machine vision system yield more accurate and reliable results [28]. Furthermore, based on the miscount data shown above, the actual accuracy of the tracking algorithm was often below 30 percent. In some approaches under-counting and over-counting over the prescribed sample interval (15 minutes) canceled each other out, which led to hourly accumulated traffic volume counts that were very close to the ground truth count measurements. Thus the hourly aggregated measurement accuracy does not represent the actual performance of the algorithm for these experiments. The success of such a tracking

system relies heavily on the camera placement. If a camera were placed more directly or high above the intersection, thus eliminating vehicle occlusion, the data would more likely match the ground truth data because blob separation from the overlapping vehicles would most likely have been better. Note the previous studies, which tested this algorithm utilizing a bucket truck, elevated the camera over 45 feet above the intersection.

Since results from video recorded were not of sufficient accuracy the existing approach did not prove to be ready for deployment with the prototype. There are no commercially available video sensors for vehicle tracking as technology is not yet mature. We used the most widely commercially available sensor (Autoscope) which was selected based on its use in by a previous study by Tarko and Lyles [28] and we developed a special logic for extracting approach volumes at intersections. This sensor already provides other traffic measurements such as volumes, speeds, headway, and classification and there accuracy has been established over the years. The methodologies developed and tested to extract approach counts utilizing this device with the field collected data will be described next. It should be noted here that operational aspects from detectors to shadow processing were designed in Autoscope with one camera per approach in mind whereby little to no occlusion exists.

The Autoscope RackVision 2004 detection system is a 'presence' detection system, which utilizes a video image-processing unit (VPU). Autoscope has user-friendly software with a basic software development kit (SDK) where virtual detectors (tracking strips) can be placed in the camera field of view in a similar manner to loops on the roadside. The virtual detectors read color and illumination of pixels in order to compare an active object on a stationary background. The hardware can then collect streaming data from the detector using the VPU to help in data collection of actuated signal timing. Newly developed detectors which track the specific movement of pixels called directional detectors, are of much use as they activate only when an object passes over the tracking strip in the proper direction. Furthermore, developed detectors collect the speed and classification of vehicles by tracking the movement of vehicles and using calibrated pixel and geometry to detect information from the pixel movement. With a

maximum of 32 overlap-able detectors per camera, a series of detection zones can be established. Furthermore, detectors can be combined into logical operations including (AND, OR, NAND, NOR, and N of M).

Upon operation, detectors, which can be visible if desired, change color when active for easy checking of proper function. Data can then be generated from active detectors to obtain volume, occupancy, headways, speed and vehicle classification. Using an internal program called 'Data Collector', interval data aggregation over a specified time period or per detection event can be obtained and analyzed.

The Autoscope machine vision system is designed for use with live or recorded video for streaming data acquisition. Presence detectors can be used across a lane of traffic to emulate the same functionality as a loop detector or along a lane of traffic for directional detection whereby only cars moving along the selected direction will trigger the detector. Autoscope hardware was designed for each video to process a single approach of traffic whereby cars moving perpendicular to traffic flow are not seen. For this reason and as the analysis to follow will demonstrate, directional presence detectors were a poor choice for detecting vehicles moving perpendicular to the primary direction of traffic flow. This implies that the Autoscope was inevitably not an ideal choice for monitoring of an intersection through non-ideal camera placement with the intent of a single camera monitoring all four approaches simultaneously. Despite such drawbacks, we designed simple, repeatable, detector configurations that generally produced accurate data extraction, which exceeded the 85 percent accuracy sought by traffic practitioners by upwards of 5 percent (approximately 90 percent accuracy thus an MPE of less than 10 percent). The following summarizes the derivation for such a detector configuration. They are compiled in the order in which they were tested with all previously collected videos. It is important to note that video collected before sunrise and dusk were not used for the automated extraction experiments because detection accuracy with unorthodox placement was already known to be problematic during these periods.

Machine Vision Volume Data Detector Configuration and Results

As mentioned earlier, the operational aspects of Autoscope from detectors to shadow processing were designed in with one camera per approach in mind whereby little to no occlusion exists. As previously mentioned volume counts were aggregated into 15-minute intervals for each approach. These counts would then be compared against the ground truth to determine the accuracy of using a single camera for the entire intersection in conjunction with Autoscope to create a vehicle counting system for all four approaches simultaneously. In order to extract such counts using only a single camera, detectors were placed in an unorthodox but strategic manner throughout the intersection as described below.

This first configuration consisted of presence detectors placed just prior to the stop-bar at each approach such that each lane had its own detector. The detectors were then attached to the detector stations (the boxes with 011 101) which then recorded the information on the data collector as described earlier in this chapter. Site 1 was used for the detector logic experiments because the intersection consists entirely of mixed thru and turning movements as well as having the fewest lanes to compare and analyze the different detector configurations and thus provided a reasonable starting data set by which to compare with the other sites.In this first configuration a baseline was established for issues that in general exist with collecting data using one camera at an intersection. From the results it can be seen that occlusion, shadows and other issues existed with this setup, as the accuracy is very poor, with a MPE of 245 percent and an R^2 value of 0.15.

Next, configuration two was tested. In this configuration, the presence detectors from configuration 1 were replaced with directional detectors. In this case, directional detectors were also placed just prior to the stop-bar such that they would extend just inside of the stop-bar. In essence a vehicle would trigger the directional detectors just as they entered the intersection. Again, each detector was connected to a station detector as

described in configuration 1.

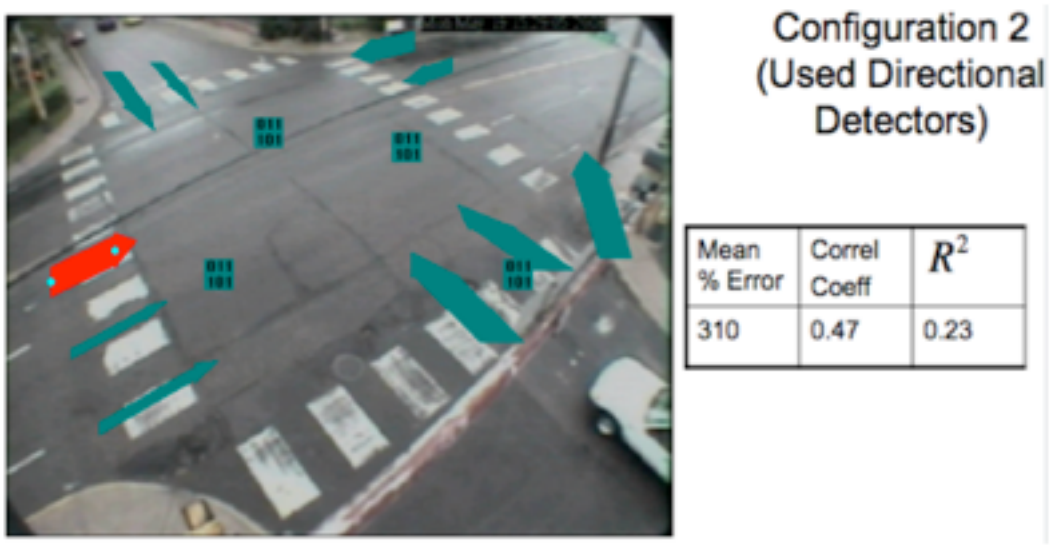

Figure 25: Site 1 - Configuration 2 - One presence detector per lane at Site 1.

On this second configuration, the directional detectors are used in place of the presence detectors in the first configuration. This setup established the accuracy with which advanced detectors performed. As the results show, shadows, occlusion and high-speed vehicles greatly limited the effectiveness of the directional detector. From watching the video process, it was visible that high-speed vehicles were the primary source of error with this configuration as the detectors failed to recognize vehicles at such a high velocity.This third configuration attempted to counter the high-speed vehicle error by placing two directional detectors in series. These detectors were placed one in front of the other starting from behind the stop bar. Oftentimes both missed the vehicle or other similar errors occurred. These errors made the detector layout and calibration process of the series of detectors very difficult and unfortunately showed little improvement from configuration 2 with still over 107 percent MPE. MAPE for this site (with this configuration) can be seen later on in Figure 33.

Configuration 4
(Optimal)
(combination)

Mean % Error	Correl Coeff	R^2
9.96	0.80	0.65

Figure 26: Site 1 - Configuration 4 - Combination of presence and directional detectors - one per lane.

In this fourth configuration, by combining both presence and directional detectors it was possible to eliminate the high-speed error of the directional detectors while maintaining the utility of the directional detector on the optional lanes and or on lanes where occlusion and opposing traffic may interfere with accurate counting. As Figure 30 shows, the presence detectors were placed even further behind the stop bar than in configuration 1 and the directional detectors were used where high-speed vehicles were less likely to be an issue such as turning lanes.

Configuration 5 (Optimal with Shadow Processing)

For all intersections combined

Mean % Error	Correl Coeff	R^2
9.86	0.81	0.66

Figure 27: Site 1 – Configuration 5 – Combination of presence and directional detectors – one per lane with shadow processing.

Similar to configuration 4, this configuration utilizes both presence and directional detectors, however, for this experiment the shadow processing system was activated and thus the MPE and R squared are slightly improved. The data indicated that the shadow processing resulted in little improvement from the previous configuration and therefore was not utilized for the other site experiments. The MAPE can be seen later on in the statistics for all approaches (see Figure 33 for MAPE of this site).

All configurations were created by a brief "trial and error" placement of detectors and observing the vehicles passing over the detector to insure each detector was detecting vehicles properly. In addition, the Autoscope calibration process carried out prior to detector layout takes into account the size of the intersection and automatically sizes the detectors. It was necessary for many approaches to increase or decrease the detector size in order to adjust its coverage area from the default. The detector placements and configurations at the other three sites accompany the results below.

Final Detector Configuration Results

The fourth configuration, which utilized single directional detectors indicated the most accurate measurements and can be set up and calibrated in a short amount of time. Below is the machine vision acquired data and a breakdown followed by analysis.

The detector layout utilizing the far lane directional detectors used at Ottowa and Minnetonka for data extraction is illustrated in Figure 31. Following each detector configuration will be the per-direction volume results for each site.

Figure 28: Site 1 - Detector configuration.

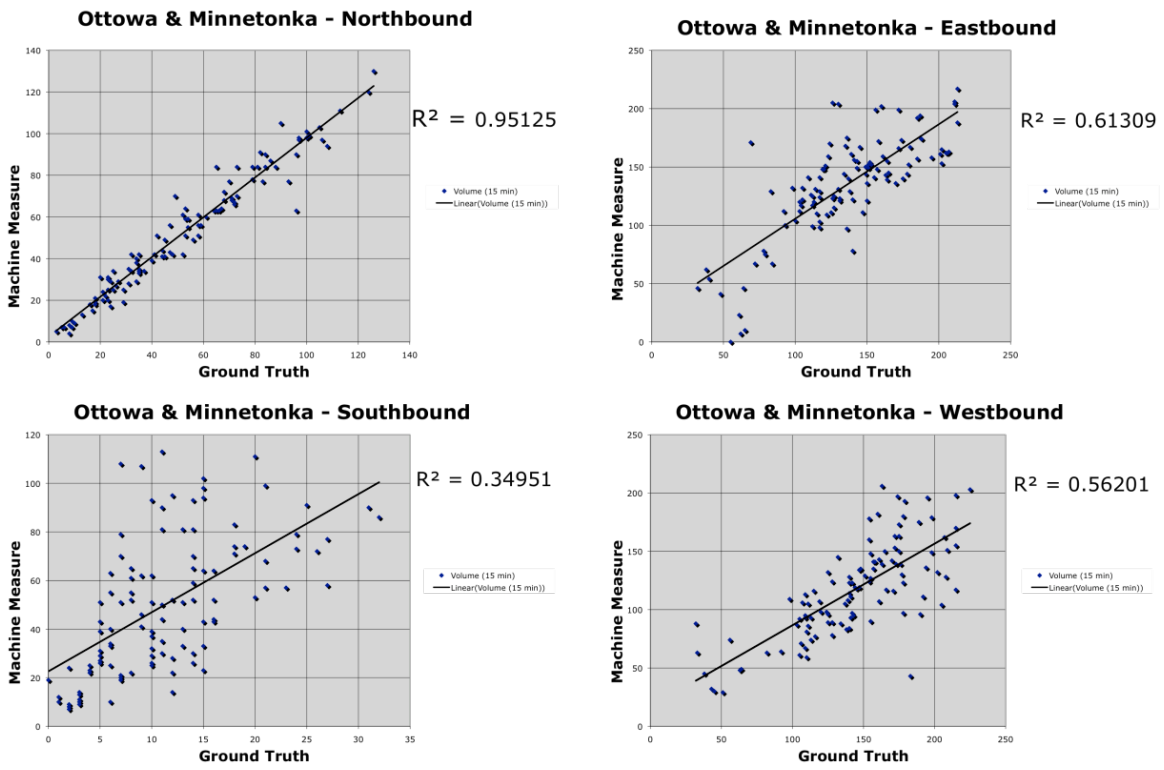

Figure 29: Configuration 4 - CSAH 5 (Minnetonka Blvd) and Ottowa Ave. - Results scatter plots (per approach).

Ottowa and Minnetonka is the first site for data extraction and thus the least difficult types of approaches. Furthermore, the intersection is smaller than the other sites and thus allows for more detail in the video (increased number of pixels per square foot). The data from Figure 32 and summarized in Figure 33 demonstrates the accuracy obtainable from the approaches nearest to the camera (northbound) and thus an R squared value near 1. The occlusion, which was later verified visually, was consistently a problem for the detectors on these approaches. What is most interesting is the error in the far approach (southbound) data which was later visually confirmed to be a detector glitch causing the occlusion errors to compound to nearly 405 percent MPE. This means that while errors from an approach a similar distance from the camera (westbound) was as high as 15.7 percent MPE and 23.7 percent MAPE, the use of directional detectors at cross traffic prone occlusion sites was the major source of the error. This specific approach will be discussed in further detail later on in this chapter.

Ottowa & Minnetonka (OM)

OM	RSQ	C C	ABS%Error	Mean %Error
NB	0.9512522	0.9753216	11.8879809	2.985640614
EB	0.6130878	0.7829992	19.1562282	0.774192894
SB	0.3495081	0.5911921	404.616799	404.6167986
WB	0.5620129	0.7496752	23.7225753	15.76012738
Total	0.6189652	0.774797	114.845896	106.0341899
Total -South	0.7087843	0.8359987	18.2555948	6.506653629

Ottowa & Minnetonka (OM)

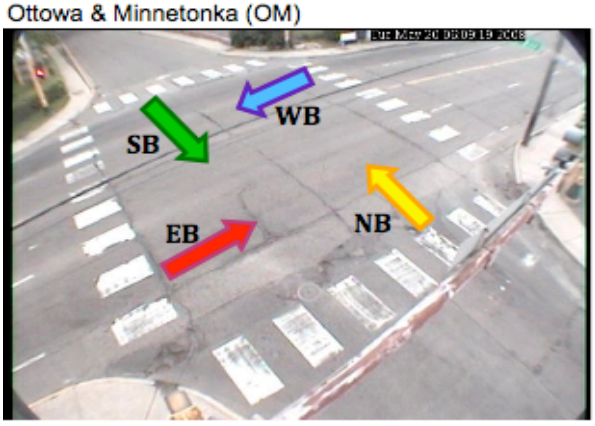

Figure 30: Site 1 - Minnetonka Blvd. and Ottowa Ave. - Ground truth comparisons for all four approaches.

The anomalous data involving the southbound approach of Ottowa and Minnetonka will be discussed in further detail later on in this section, however, it should be noted that the MPE of the intersection as a whole was only 6.5 percent, which is within an acceptable range according to practitioners.

Next is the intersection of Louisiana Ave. and Minnetonka Boulevard (Site 2), which is slightly larger in geometry than Site 1 and with a slightly more complex approach configuration. At this intersection there are clearly defined turning lanes and again, by placing detectors just prior to the stop bars, the accuracy was improved from the original configurations as described earlier. Occlusion and shadows were a major concern at this intersection, which could not be easily mitigated with the developed detector configuration. The result was a pattern of both slight over and under counting. The

southbound approaches (upper left hand corner of image with movements toward the camera) experienced large over counting. The reason for this will be discussed later.

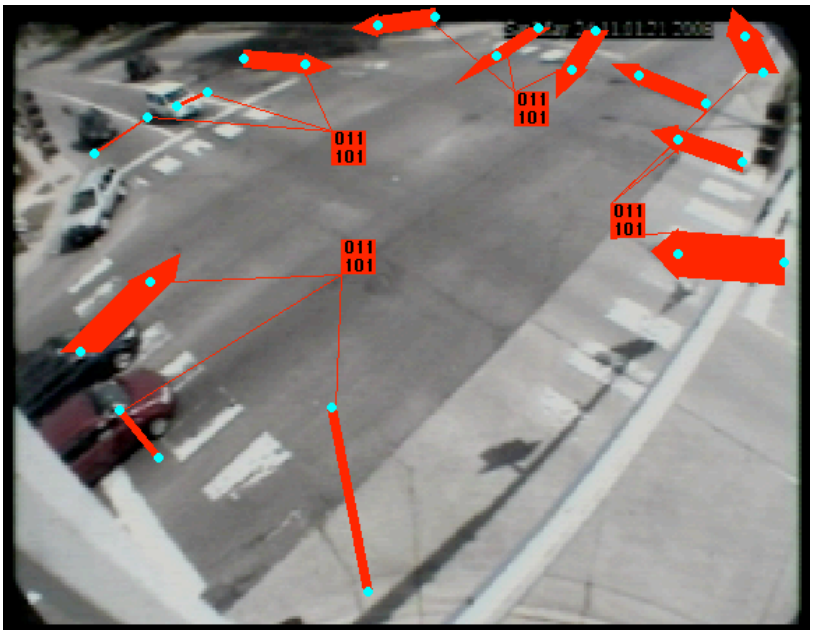

Figure 31: Site 2 - Detector configuration.

The above detector configuration shown in Figure 34 yielded the results written and analyzed below which show a pattern of both slight over and under counting for the other intersection sites as well. Issues in accuracy using the above detector configuration were likely attributed to shadows and occlusion; however, it is unlikely that 'trip-wire' type machine vision systems can improve on such accuracy due primarily to occlusions and cross-lane shadows.

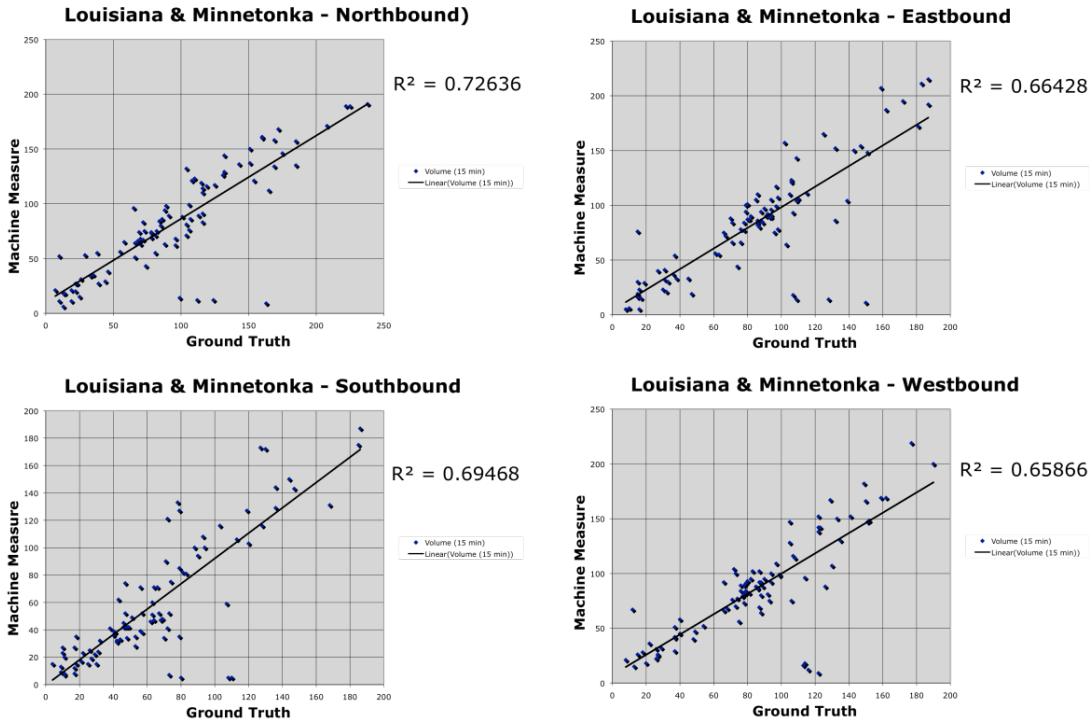

Figure 32: Configuration 4 - Louisiana Ave. and Minnetonka Blvd. - Ground truth comparisons for all four approaches.

The above figure (Figure 35) shows the volume data points per 15-minute interval, which were collected at each approach using the above detector configuration. While the R squared values are not ideal (values of 1.0), the mean percent error, which is commonly used in conjunction with traffic signal optimization, is low in percent error and shown below (Figure 36). This means the data collected would have significant advantages to traffic engineers responsible for optimizing traffic signal timing.

Louisiana & Minnetonka (LM)

LM	RSQ	C C	ABS%Error	Mean %Error
NB	0.7263604	0.8522678	26.2459521	2.514386261
EB	0.664281	0.8150343	25.4740943	3.913851546
SB	0.6946829	0.8334764	31.8978267	1.77169683
WB	0.658655	0.8115757	24.8268032	10.04351475
Total	0.6857307	0.8280886	27.1111691	4.560862348

Louisiana & Minnetonka (LM)

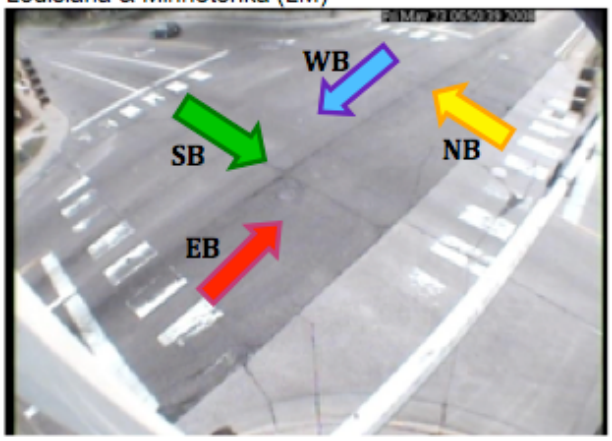

Figure 33: Site 2 - Louisiana and Minnetonka - Ground truth comparisons for all four approaches.

As show above in Figure 36, the mean absolute percent error (MAPE) and mean percent error (MPE) are significantly different. This means the error per data point found was both below and above the ground truth data. Such errors can be attributed to glitches in the detectors. We visually confirmed that these errors were caused by shadows, closely following vehicles and 'glitches' in the detectors (phantom counts and other seemingly random miscounts).

Below is the detector layout used on Snelling and County Rd B. While very basic in design, we found that increased detectors only hindered the accuracy of the volume data that was collected. It is clear from this layout that while near to the camera approaches were able to utilize presence detectors only, far approaches required directional detectors.

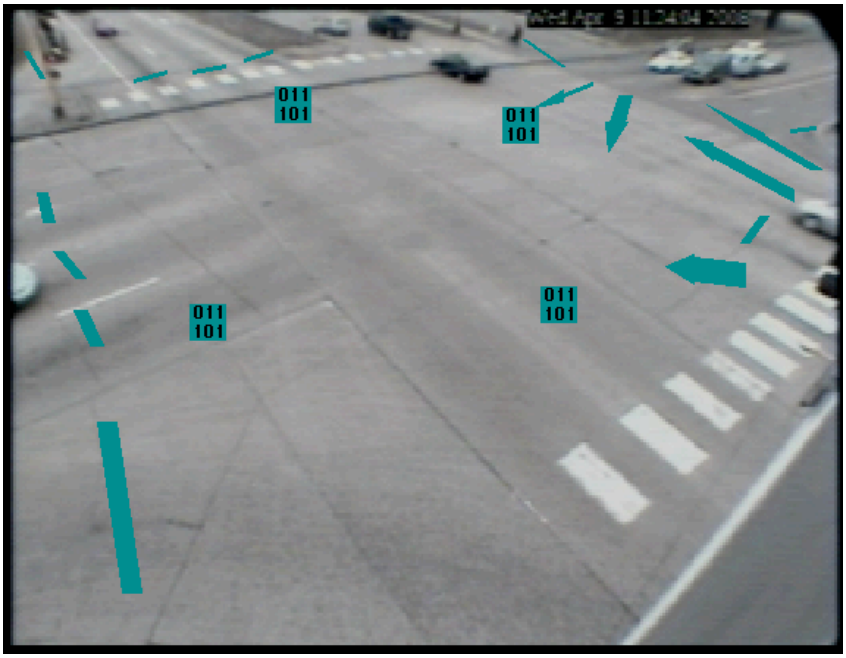

Figure 34: Site 3 - Detector configuration For Snelling & County Rd B (Site 3).

Given the glitches seen in directional detectors from the previous configurations we expected that more error would occur in approaches that used such directional detectors. Errors persisted despite attempts to combine the use of directional and presence detectors on these approaches. Furthermore, use of both directional and presence detectors became hindering to the accuracy because presence detectors gave many false positives and directional detectors missed vehicles all together. The extracted traffic count errors at this site were consistent with the previously discussed occlusion analysis which predicted occlusion would be more pronounced on the far lanes particularly when viewed from the corner of the intersection.

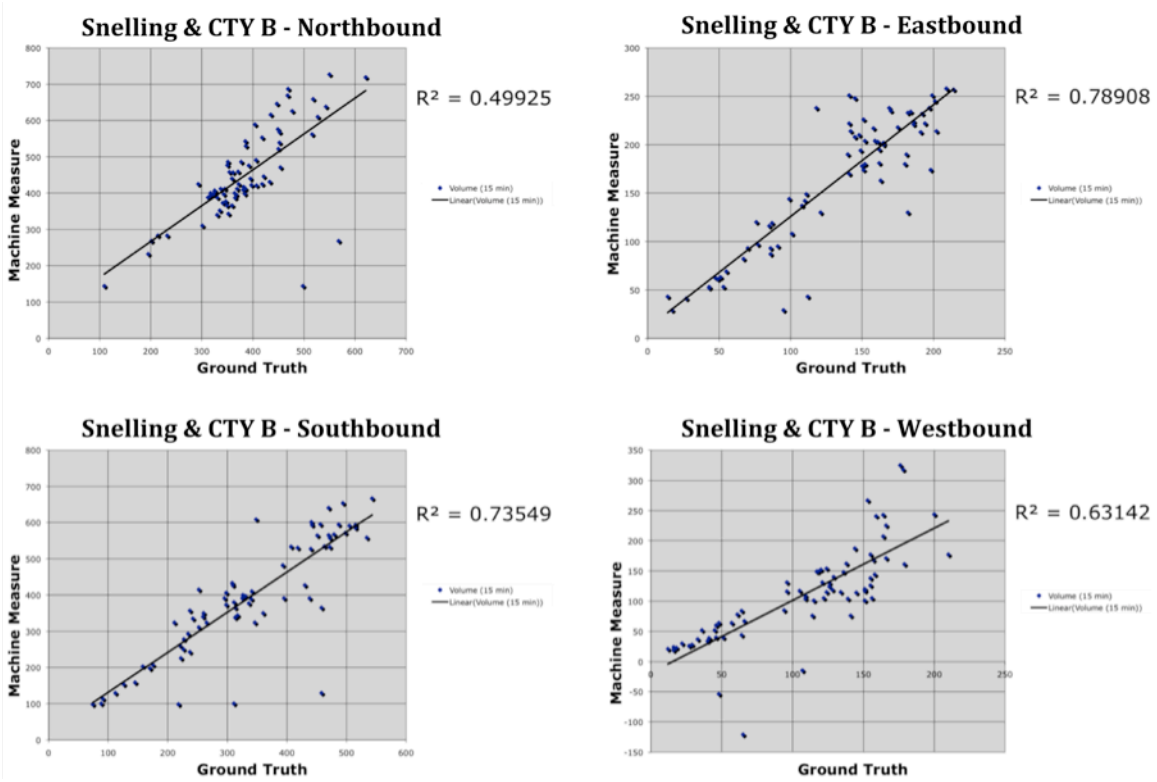

Figure 35: Site 4 - Snelling and County Road B - Ground truth comparisons for all four approaches.

There are fewer data points from this intersection than the other sites due to weather and extreme wind issues experienced during while deployed at the site. These situations created conditions whereby no reasonable data could be obtained. On one day in particular, the weather caused the camera to fog and no data was collected. This was due to a small leak, which formed in the protective housing for the camera, which was later repaired.

A pattern seen in the errors shown above (Figure 38), demonstrate that with higher volumes, there was also larger error. Such a pattern is expected to stem from closely following vehicles. This means that the detectors failed to reset between each vehicle and thus double counted vehicles or miscounted them when shadows could be seen. Visible confirmation of these errors shows occlusion to be a major source of error, one that can only be fixed through better data acquisition techniques and or the use of

tracking the vehicles such that moments of occlusion do not confuse the detectors and create error.

Snelling & CTY B (SC)

SC	RSQ	C C	ABS%Error	Mean %Error
NB	0.4992507	0.7065767	21.3672801	17.7409958
EB	0.7890772	0.8883002	31.8807616	26.97294822
SB	0.735493	0.8576089	24.1852168	17.42497808
WB	0.6314185	0.7946185	31.235981	0.520503122
Total	0.6638099	0.8117761	27.1673099	15.6648563

Snelling & CTY B (SC)

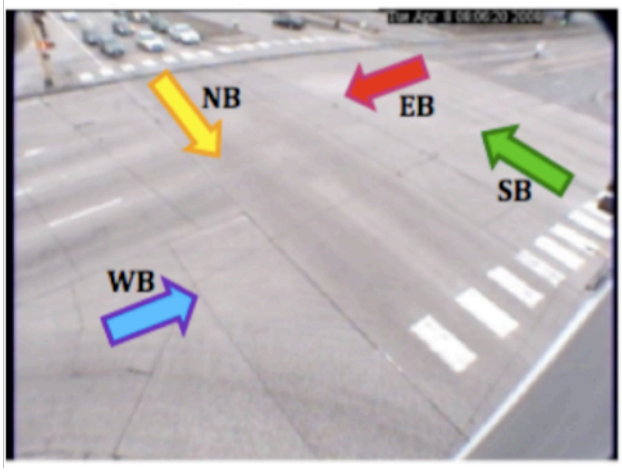

Figure 36: Configuration 4 - Snelling and CR-B - Results (per approach).

The above data is important in revealing the source of errors in the volume counts. Most importantly, the westbound approach (nearest to the camera) had a very high mean absolute percent error (MAPE) and a very low mean percent error (MPE) thus as was confirmed visually, a pattern of occlusion and shadow errors are the primary cause of the errors and not the directional detectors because this approach did not use directional detectors. This demonstrates the difficulty to obtain accurate counts at large intersections with a single camera where the pixel resolution is inadequate to discriminate between vehicles in the foreground and the background. To be sure, is can be inferred both visually and from the data that with two cameras, the accuracy would be vastly superior

given only the two near to the camera approaches would need to be detected by each camera.

Below is the detector layout for Site 4, Hwy 252 and 66th Street. The blue and red detectors were colored for the sake of visibility and were not different than any other directional detectors. Here it is evident that only directional detectors could yield data given the size of the intersection and thus the potential for occlusion. By placing the camera on the median, the occlusion was minimized particularly on the mainline approaches. However, the result of this deployed location is the inability to observe and thus detect some of the lanes on the eastbound and northbound approaches (the top of the screen is north). Therefore, while some data was missing due to the camera placement, the extracted measurements were improved by the resulting camera vantage point at this location. Below is a summary of the findings.

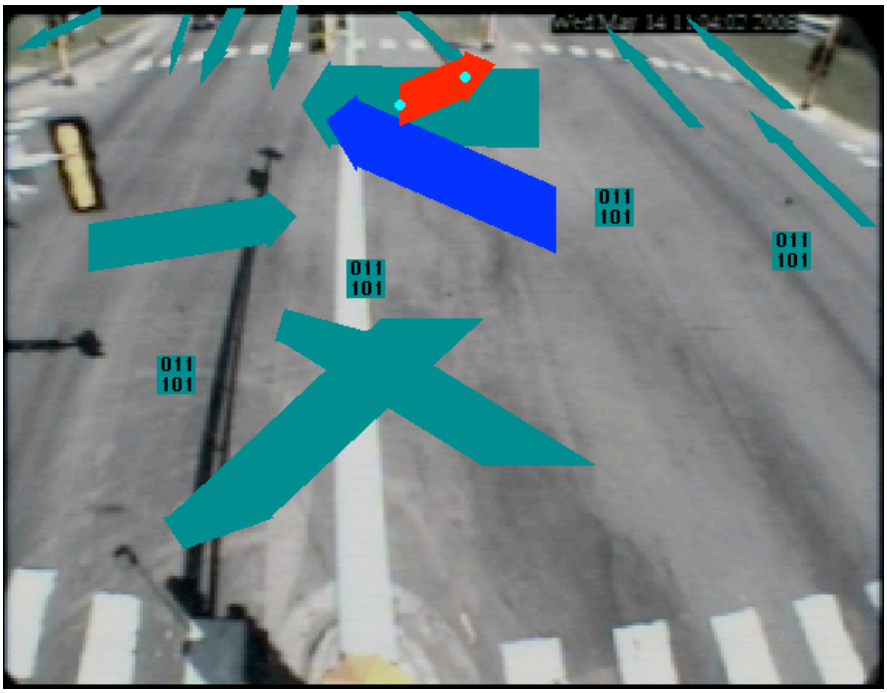

Figure 37: Site 4 - Detector configuration.

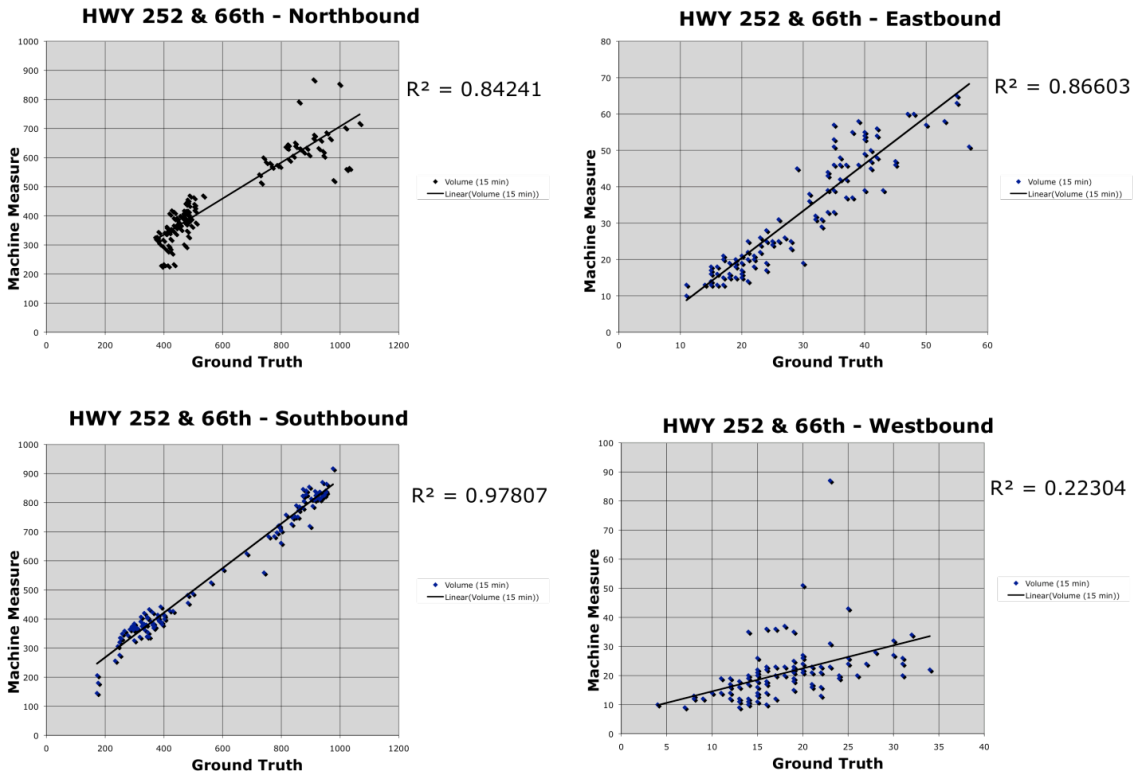

Figure 38: Configuration 4 – HWY 252 and 66th St. – Results scatter plots (per approach).

This data, excluding the westbound approach, which will be discussed below, showed high detection accuracy. This can be attributed to the minimization of occlusion and thus the increase in visibility of vehicles traveling through this intersection. The directional detector errors observed at Site 1 (Ottowa and Minnetonka (CSAH 5)) southbound approach was again observed in the Site 4 HWY 252 and 66th westbound approach. The data therefore suggests a systematic error with this type of detector rather than occlusion or other factors. With exception to the eastbound approach, the extracted traffic measurements appear to be accurate and despite high-density traffic, occlusion errors seemed to be minimal and are summarized below (Figure 42).

HWY 252 & 66th (25266)

25266	RSQ	C C	ABS%Error	Mean%Error
NB	0.9780672	0.9889728	12.3262103	2.574053633
EB	0.8660337	0.9306093	16.8423729	7.571206935
SB	0.842408	0.9178279	21.7255654	21.72556541
WB	0.2230381	0.4722691	32.0996514	20.70129919
Total	0.7273868	0.8274198	20.74845	13.14303129

HWY 252 & 66th (25266)

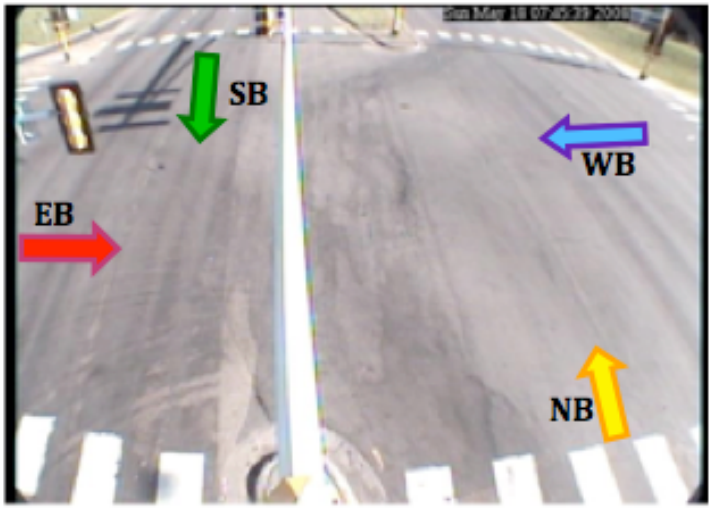

Figure 39: Configuration 4 - HWY 252 and 66th St. - Results (per approach).

At this intersection, the approaches all used directional detectors rather than presence detectors. Due to the size of the intersection and the high speed of vehicles, such detectors did not encounter occlusion and thus the issues causing error were not present. As a result the accuracies were high.

Directional Detector Error

Substantial errors impacted the Site 1 (Ottowa and Minnetonka) – Southbound (SB) approach (OM-SB) on the aggregate data for all intersections which is highlighted by the

red arrow on Figure 43. Several experiments in which we adjusted the location and direction of this detector did not reduce this particular error. Again, as stated after the Site 3 results, two cameras would greatly reduce this error as a second camera would count the two farther approaches and as the data reveals, these 'far' approaches were the source of most of the error. Interestingly the glitch in the directional detector for the other site approaches was not nearly as revealing as this particular case. For this reason it was important for volume accuracy to be calculated with and without this approach data so that the overall system accuracy and the potential accuracy if the glitch were fixed could be seen and highlighted.

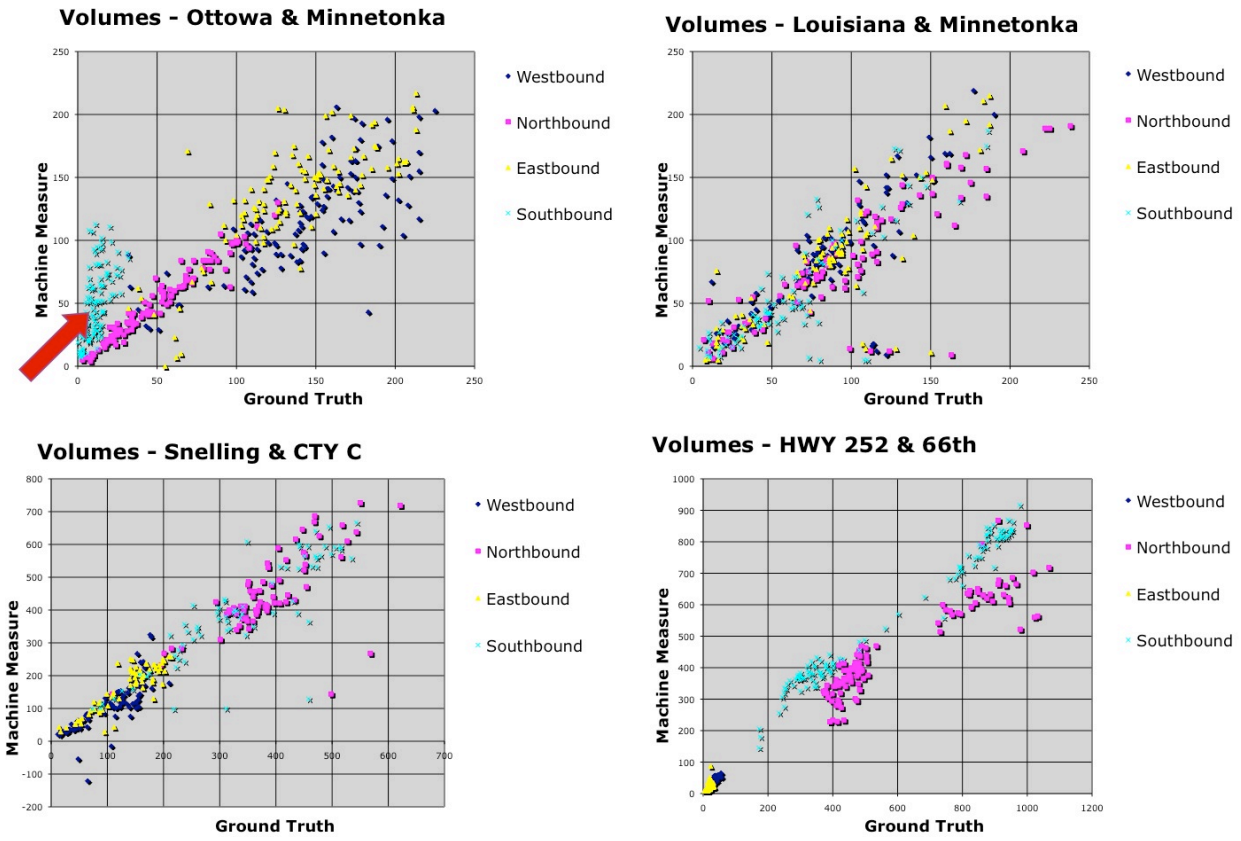

Figure 40: Extracted volume counts of each intersection.

The approach volumes extracted from the machine vision system are generally well correlated with the ground truth measurements described previously. As shown in Figure 43, the exception was the southbound (SB) approach at the first site, Ottowa and Minnetonka. If this single approach is removed, the MPE falls under 10% (Table 6).

While it can be seen that errors occur on all approaches, the overall accuracy was acceptable and in accordance with the previously described functional specifications.

Table 8: Aggregated results for the four intersection sites.

	R^2	Pearson R	MAPE	MPE
SB site 1 approach included	0.7096	0.8105	47.47	34.85
**SB site 1 approach removed	0.7320	0.8258	23.32	9.97

Table 8 indicates the aggregate error for all sites and approaches for any 15-minute count was slightly less than 10% while the average error was less than 25%. Note that the MPE and MAPE statistics are very sensitive to outlier errors. For example, the large over counting errors experienced for the single southbound approach created an MPE which was over three times larger than excluding this approach (34.85%) and a MAPE which was essentially twice as large.

In this chapter automated extraction of volume counts was developed and analyzed. The results demonstrate that a combination of presence and directional detectors can accurate detect and collect volume counts. Directional detectors occasional gave spurious results that contributed significantly to the measurement error. In principle, directional detectors can be used to extract turning movements as well [20]. It seems reasonable that the anomalous behavior of this type of detector may be due to inherent design issues in our detector layout or software algorithms, as they have not been tested in a manner presented herein. We surmise that even modest improvements in direction detector accuracy and the use of a second camera will significantly improve counting accuracy.

Measuring directional movements from thru and turning vehicles is feasible with multiple cameras or once a panoramic view of the intersection with minimal occlusion is established, using special detectors available in Autoscope, a kinematic algorithm was designed to detect through and turning movements at all approaches. Using a combination of directional and logic detectors found in Autoscope, vehicle movements were tracked correctly. When access to the controller cabinet is feasible through either wireless networking with an Autoscope in the cabinet or through attaching the apparatus

directly to the controller cabinet (using the cabinet as the mount-to infrastructure), Autoscope can extract phasing states alongside the video detectors. Knowing the current phase allows decisions to be made about where cars are coming from and where they are going to in combination with the kinematical algorithms even more accurately. The standalone requirement during deployment at these intersections prevented us from obtaining phase information from the intersection control cabinet. Without the phase information it became extremely difficult to utilize our previously described Autoscope kinematic algorithms to determine turning movements, which was made only more difficult by the ability to record with only one camera view at a time. As a result a phase detector was created based on a second kinematic algorithm for detecting the active phase; however, it was found that even minimal errors on the part of the kinematics phase detector lead to large error on the part of the turning movement identification and counting technique. As a result, even though most of the data collected was visually accurate upon observing the algorithms run, the few random algorithm errors lead to large data errors and thus the majority of the data counts were inaccurate. For example, during congested periods (which represents the majority of video collected) it was found that the volume of straight movements during a single cycle was equal to or greater than the volume of a turning movement for an entire 15-minute period; thus a single phase detection error during a cycle would cause a turning movement count to nearly double in size. This can be corrected if the directional detectors in Autoscope are adjusted to apply to non-through vehicles or if access to the controller becomes available. A request for this modification has already been requested to the sensor developers and is currently planned for future modification. Access to the controller on the other hand is feasible and is currently planned.

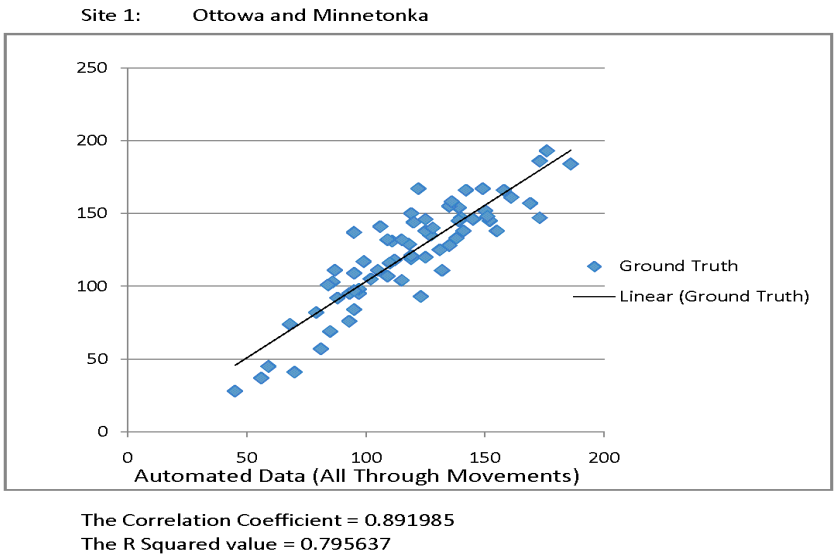

Figure 41: Ground truth vs. measured thru and turning volumes at all approaches of Site 1.

It should be pointed out that as Figure 44 (above) demonstrates, straight movements were not seriously affected by the occasional error in the detection of the phase because of their magnitude as explained earlier and thus vehicle movements could be accurately measured. The next section will describe a mid-block arterial deployment experiment to analyze extracting speeds and vehicle classifications.

J. Arterial Mid-Block Data Acquisition

In order to test the ability of the prototype to extract speed and vehicle classifications, a mid block experiment was performed. In this experiment volume, speed and classification were tested in one direction covering three lanes. Calibration was performed and speed detectors were placed on each lane. Straight-line distance measurements were done on-site at down lane and cross lane locations, which could be seen though the camera view seen below. Each position is displaced at a relative distance of 25 feet. The known displacements were use to directly measure space mean speed as previously described.

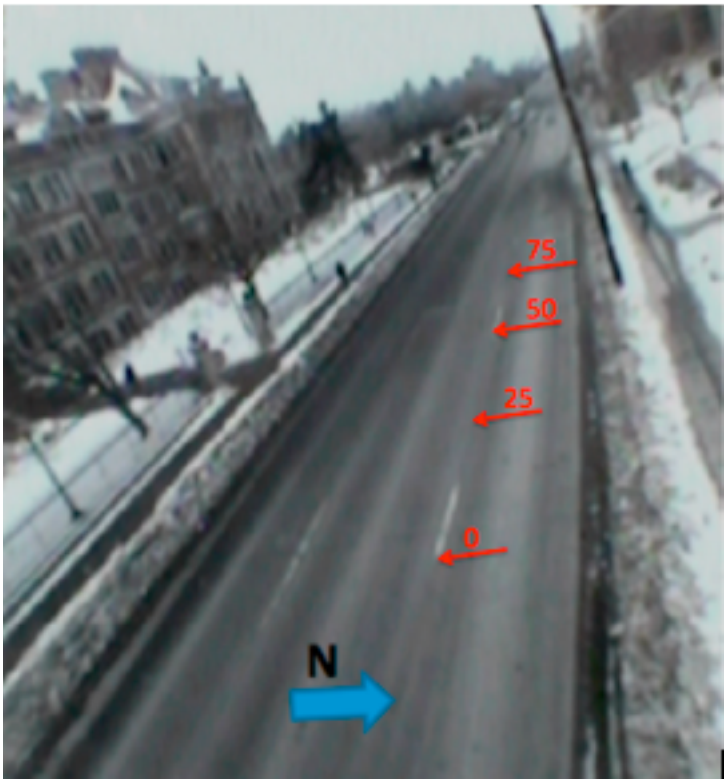

Figure 42: SE University Ave. and SE 17th Ave. with labeled distance markers indicated.

Arterial Mid-Block Data Results And Analysis

The speed data collected for all three lanes plotted against the ground truth measurements is shown in Figure 46. The far lane is most likely to have occlusion issues and one would expect that the far lane would also have the worst accuracy as it is farthest from the camera. The results below break from such a hypothesis and instead paint a picture of fallibility of the speed detector.

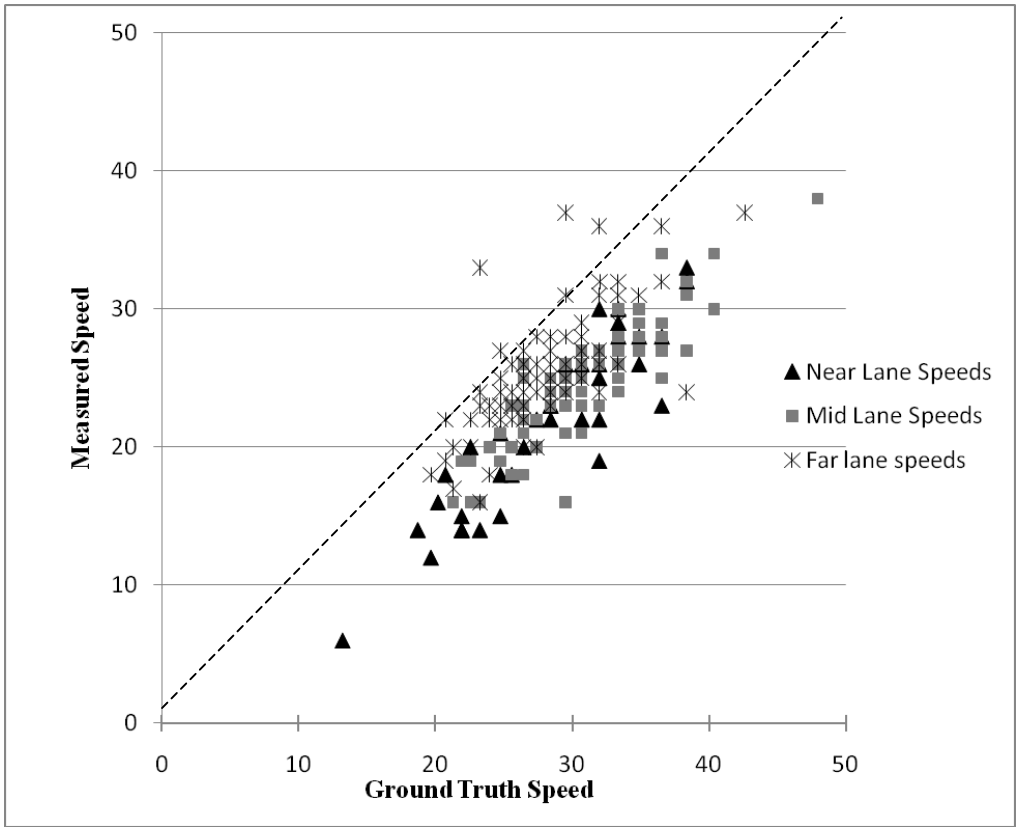

Figure 43: Measured speed data vs. ground truth measurements for the near, middle and far lanes of traffic.

The consistency of underestimate of measured speed, which would suggest the issue, lies in the calibration on the speed detectors. Autoscope speed testing results demonstrated a wide range of inaccuracy. For example, MPE ranged from about 9 to 24 percent and Pearson's R ranged from 0.74 to 0.91. This inconsistency can be attributed to calibration error, which can be fixed by improving the calibration algorithms. In turn, this calibration issue also affected the classification as shown in Table 10.

Table 9: Mid-block speed data (per lane).

	Far lane	Middle Lane	Near Lane
Pearson R	0.7358	0.8554	0.9107
R^2	0.5414	0.7317	0.8294
MPE	-8.80	-19.23	-24.24
MAPE	11.04	19.23	24.24

Table 9 reveals two trends. The Pearson's correlation coefficient shows us that actual and measured data correlated better when the vehicles were closer to the camera. This result is consistent with the occlusion analysis presented earlier. The second pattern shows that the MPE error decreases as distance from the camera increases. This is the opposite of what we expected, as from our previous experiences, distance and error increase with a direct proportion, given the farther from the camera the object the harder details are to capture. Over-estimating speed was commonly seen in the near lane detections but not as frequently seen in the middle and far lane detections. This demonstrates a trend in the machine vision, which is not consistent with calibration errors but rather a trend, which is inherent in the machine vision detection algorithm.

Table 10: Mid-block classification data.

	Class A	Class B	Class C
Sample Size	223	11	11
Measured Accuracy	96.86%	4.64%	3.63%

The Autoscope machine vision system separates vehicle types by estimates of vehicle length and not axle distance. The results from categorizing three vehicle classes (A=private vehicles, B= trucks/RVs, C=heavy trucks) determined that the tested machine vision system was accurate at normal vehicle classification (A) but much less accurate at uncommon classification such as trucks and buses. The inaccuracies seen in the classification of vehicle types B and C are likely the result of vehicle occlusion, insufficient calibration and small sample size.

Certain environmental and unavoidable conditions hindered data collection to such an extent that they were removed from the data pool altogether. When these conditions,

which are listed below in detail were present, the data was logged and visually analyzed but not used in the experiments.

1) Extremely low lighting conditions. These were found during day to night transitions (dawn and dusk).

2) Rain and extreme fog. All of these hinder accuracy on detection, most notably rain and extreme fog. Of these, none occur during normal data counts as such data is irregular and has no utility to traffic engineers.

    a. Snow – both standing and falling snow hinder accurate background recognition.

    b. Sleet – Similar to rain, it caused false headlight recognition

    c. Rain – Caused 'doubling' of headlights and glare, rain is a primary source of detection error

    d. Extreme fog

    e. High winds – caused occasional 'Phantom' detections due to moving background image triggering the detectors.

3) Incidents. (Stalled vehicles or accidents). Normal traffic conditions do not exist and normal vehicle movements are altered thus rendering sensor locations ineffective.

4) Initialization Periods. The beginning of each video clip requires ample time for the background to render and thus accurately detect.

The data collected during these conditions was initially analyzed and compared with the ground truth data but it was evident that such data was simply random and without utility to our experiments or transportation practitioners. It should be understood that these conditions help define the limitations of Autoscope for this application.

K. Queue Length Detection Study

On average over the last five years, there have been over 1,150 roadside work-zone related deaths. In 2002, Mohan and Guatam estimated over 26,000 lost day injuries resulted in a total cost of $2.46 billion alone, which according to the U.S. Treasury department, equates to over $2.82 billion in 2008 dollars, not including the enormous cost of potential injury liability [29]. Highway work-zone fatalities per billion dollars spent cost at least four times more than in total U.S. construction. This is in spite of recent advances in developing WZITS safety systems as a safety counter measure to mitigate such grievous situations. Many of the crashes occur when drivers encounter the queue tails in the vicinity of the active work-zone and are unprepared to stop. Adding queue length detection to WZITS's will improve detection of dangerous traffic conditions near the active work-zone thereby allowing the WZITS to provide more accurate critical warning information to drivers. Furthermore, implementing the queue detection on a low-cost rapidly deployable device will make utilization of WZITS more attractive especially for more temporary work-zones where utilizing more invasive and costly radar and or trailer-based systems may not be practical or justified. Note that a near active work-zone area queue detection warning systems does not exist.

The final field experiment tested the feasibility of a detector algorithm developed to extract queue lengths from the video data. For real time situations, knowledge of the queue length can increase travel times along corridors as actuated traffic signals can be better optimized using this information. Such optimization can occur from further extending the effective green time when queue lengths exceed a threshold length. Specifically, the queue size can be estimated given average headways and thus only relinquish signal priority after queue lengths decreased past a given threshold. Extracting queue length propagation in real-time can also be used for traffic safety operations. For example, active work zones on arterials can be made safer through intelligent warning systems that utilize the knowledge of queue tail locations, which are in close vicinity to the actual construction activity area in the work zone**.**

Figure 44: Site 6 - Queue approach.

As can be seen in figure 47, queue lengths beyond approximately 500 feet from the placement of the portable device will not be detected due to lack of visibility (back of the clearing on the left of the image). The focus of this implementation is to detect traffic speeds and the resulting queues near work-zone areas, as a crash caused by the queue tail beyond this distance will less likely intrude upon the active work-zone. The algorithm tested is described next.

Queue Length Detection Algorithm

In theory placing many presence detectors and carefully watching occupancy and the speed of vehicles as they pass over the detectors would generate information about effective queue lengths. Implementation of this theory proved unrealistic as both the

accuracy of speed data and the limitations of detector accuracy as distance from the camera increased rendered design of the system impossible. The distance from the camera decreased the number of pixels that defined a vehicle, and inevitably prevented the detectors from differentiating a vehicle from the area around it. To address this issue, both speed information and individual vehicle recognition were disregarded, and instead the algorithm consisted of a real-time regression ladder approach, which utilized Boolean logic (logic operations) and occupancy alone for calculating a more incremental but far more consistent effective queue length detection system. Furthermore, the queue length detection was done as a-per approach detector set rather than a per-lane in order to minimize occlusion and pixel resolution errors. Here, the effective queue length signifies the queue length from the stop bar/ queue origin location. The reasoning for using a predetermined queue location is that objective is to detect the queue length propagation relative to an active work zone given a queue location origin location and thus a level of risk to workers for high threat collisions; and the queue would thus grow upstream in relation to the work zone area.

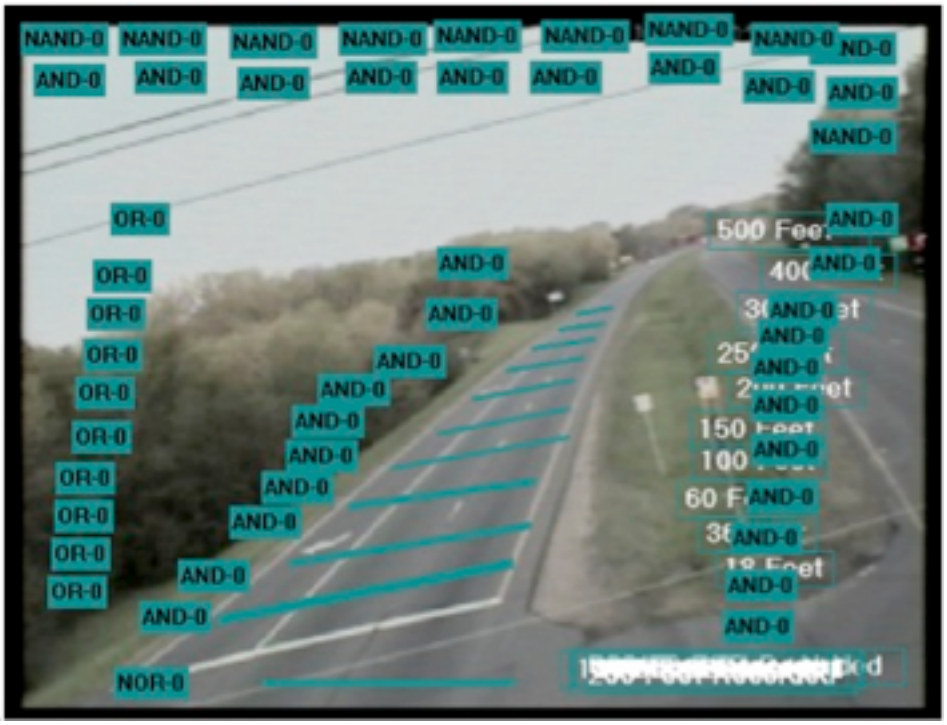

Figure 45: Site 6 - Queue Length Testing Configuration (Regression Algorithm from the Autoscope SDK).

Figure 48 indicates the locations of the 'ladder' of trip wires used to detect queue length. The horizontal bars are presence detectors, which are triggered by vehicle occupancy. The time required for these presence detectors to be triggered as active by defining when a vehicle is 'stopped' over the detector rather than passing/driving over the detector must be determined. This trigger-delay time in seconds for the detectors is denoted t_d.

Figure 49 illustrates the queue detection algorithm. Each presence detector m_j is attached to a state-machine, which is used to alter the delay time t_d. The "1" output of the state machine (a particular condition of the machine) function is attached to an AND-Boolean logic function, which is attached to the AND-Boolean logic function of the previous detector, m_{j-1}.

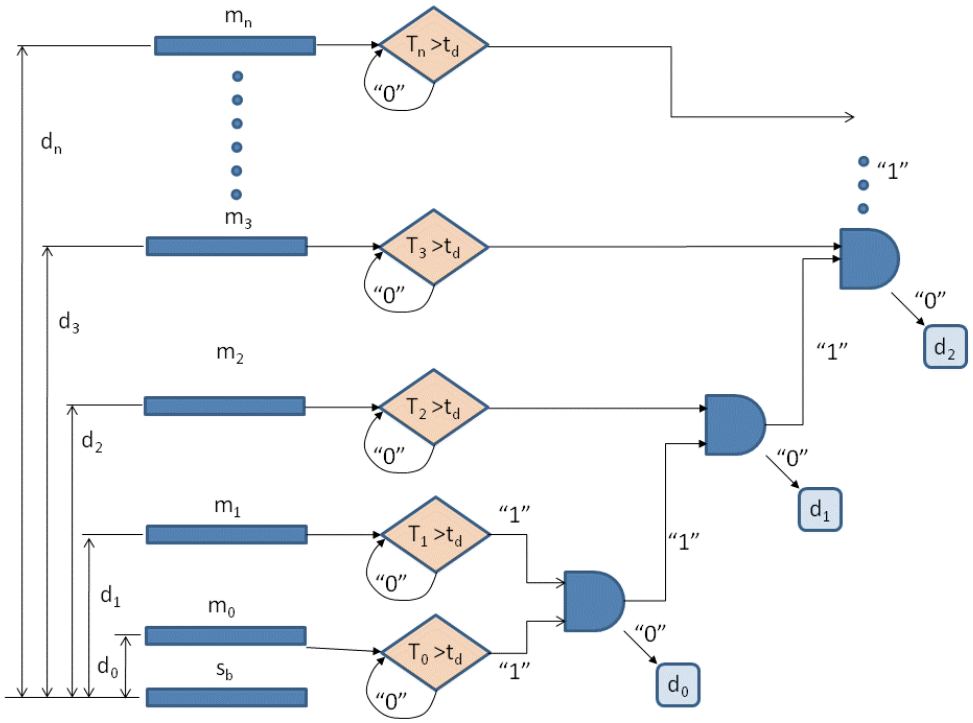

Figure 46: Queue detection algorithm using 'triggered' presence detection.

The location of the stop bar at the intersection is represented by S_b for this experiment. A presence detector was also placed at this location to 'trigger' a queue dispersion event.

Queue Length Detection Results and Analysis

Ground truth measurements of queue length were obtained at the point when the first vehicle crosses the stop bar at the beginning of the green phase. This event was emulated with the detection algorithm by placing a presence detector at approximate location of the stop bar. The logic for obtaining the queue length state is given in figure 48. The AND functions as shown in figure 49 are then attached to a series of functions for displaying the recorded queue length at the moment the queue origin location is cleared. The queue origin location detector S_b is placed in front of the stop bar location inside the intersection. A NOR-Boolean logic function is attached to this detector instead of an AND function (figure 48). Then, many trial values for t_d were run to compare the relative accuracy with respect to the ground truth model in order to determine an optimal t_d value.

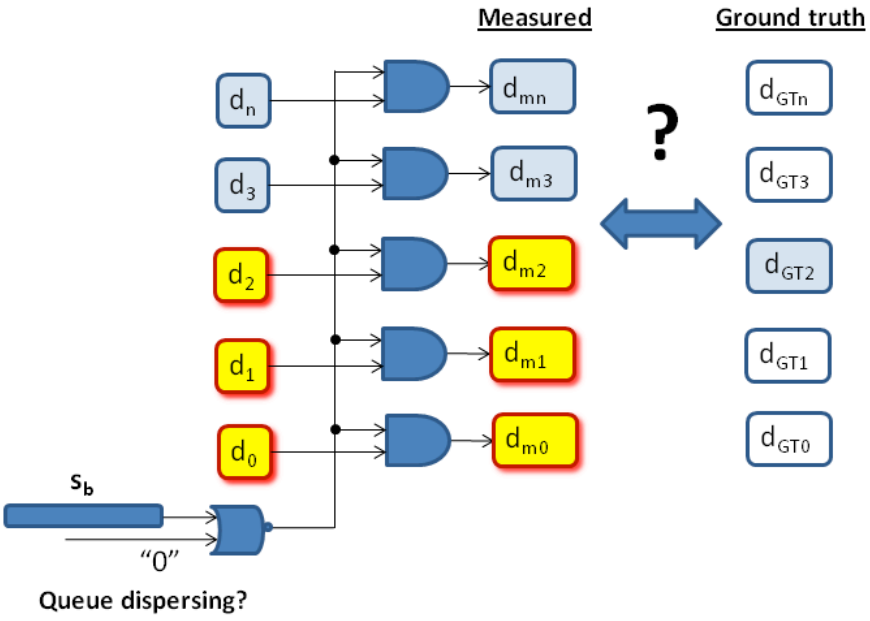

Figure 47: Queue length measurement from algorithm obtained from beginning of queue dispersion.

Table 11 reveals a minimum at approximately $t_d = 2.0$ seconds for this site agrees with the ground truth values over 96% of the time (MAPE = 100% - 96% ~ 4%). A graph of these results is shown in figure 41.

Table 11: Site 6 - Queue length data results.

61 Unique Queues Tested		
Trigger Delay time $_t$	Percent (%) Accuracy	MAPE
0.5 Seconds	77.04918033	22.95081967
1 Second	77.04918033	22.95081967
1.5 Seconds	85.24590164	14.75409836
1.8 Seconds	88.52459016	11.47540984
1.9 Seconds	86.8852459	13.1147541
2 Seconds	96.72131148	3.278688525
2.1 Seconds	90.16393443	9.836065574
2.3 Seconds	88.52459016	11.47540984
2.5 Seconds	88.52459016	11.47540984
3 Seconds	83.60655738	16.39344262
3.5 Seconds	72.13114754	27.86885246
4 Seconds	70.49180328	29.50819672

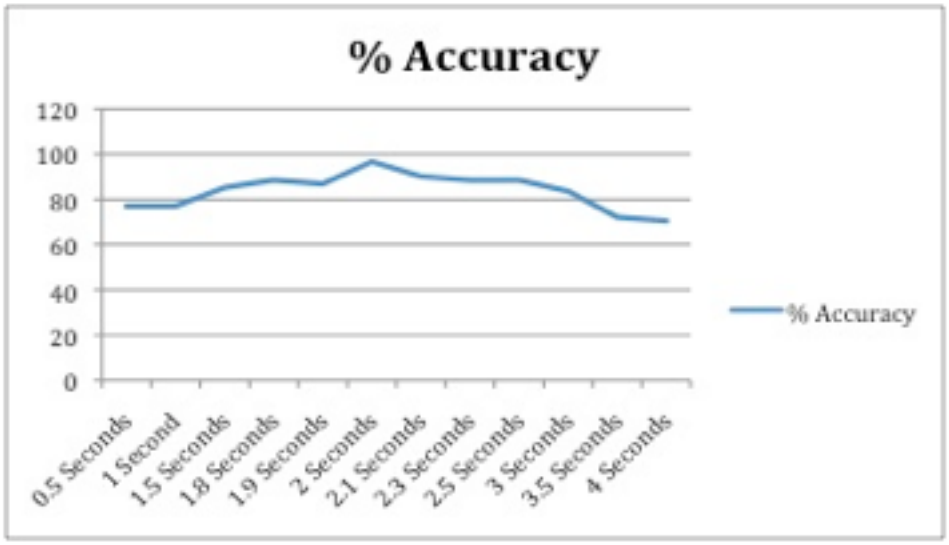

Figure 48: Site 6 - Queue length results - Percent accuracy.

Figure 51 reveals a maximum accuracy of 96.7% when t_d=2.0 seconds. The results of this experiment support obtaining accurate queue lengths up to 450 ft with the current apparatus within 4% error as compared to ground truth measurements. In this case 'ground truth' queue length was measured once per cycle at the beginning queue dissipation.

L. Conclusions

To conclude, a system for easily deployable, non-intrusive, portable, low-cost device designed for traffic data collection and video recording was designed, developed, and field deployed for over 106 hours under all weather conditions. Traffic information necessary for signal optimization was extracted from our hardware by incorporating and deploying machine vision sensors to work in conjunction with our apparatus. With topology analysis, and video medium, intersection design has been represented. Taking into account factors such as vehicle occlusion, environmental lighting and peak hour scheduling, sensors for extracting traffic data were tested along with vehicle tracking techniques.

The hardware design meets all functional specifications including cost, reliability and deployment according to transportation practitioners consulted during this project. The automatic data extraction component is not as accurate as envisioned as of yet, however, as video and other advanced non-intrusive sensors such as radar technologies continue to develop, data will become more accurate. To be sure, such technologies have improved dramatically over the last several years and are increasingly being used in practice. More importantly, these sensors are being enhanced with vehicle tracking technology, which should dramatically improve turning movement, speed and classification measurements.

The automated extraction of thru and turning movements was tested with a commercial 'trip-wire' based machine vision system, and an available "blob-based" tracking algorithm developed at the University of Minnesota [30]. In order to evaluate the performance, video data was ground truthed by logging approach counts with a Jamar field data collection counter. Volume data was collected and analyzed using the 106 hours of video collected at the four unique intersections. Though calibration of the machine detection systems and if necessary, detector placement, volume counts were collected at intervals of 15 minutes. The results of the volume data collection were found most accurate on manual counting through the video files, however, manual counting required more collection time (real time data collection plus some intersections required

two passes to collect the entire intersection) than any other testing, needed the most man-power and thus had the highest residual cost. For the camera positions that are feasible to obtain with the device prototype, accuracy of the tracking algorithm was far below the recommended 90 percent threshold for accuracy set by practitioners; however, the tracking algorithm had only a small residual cost. Machine vision was accurate enough to meet the 90 percent threshold where errors ranged from occlusion, to lighting conditions to detector error and additionally machine vision had a low residual cost as compared to manual counting, thus showing the most potential out of the systems tested in this study.

Classification was tested in a similar fashion as traffic volume counts at a mid-block location approximately 250 feet upstream of a signalized intersection. Given limitations in the tracking algorithm used in our study, the classification testing was only performed for machine vision using Autoscope. Such testing was performed on a per-vehicle basis after calibrating and placing speed detectors as described in the Autoscope user manual and then attaching detector stations for acquisition of classification information. While the accuracy of small vehicles (A) was good (above 95 percent), the larger two classifications (B and C) had significantly larger errors with results showing accuracy below 50 percent. It should be further noted that the mid-block testing met the conditions of Autoscope's normal use, however, classification was not also tested with the stop bar installation type.

Speed testing, similar to classification testing, was also performed at a mid-block location and was only tested with the Autoscope machine vision system, as the tracking algorithm output did not provide speeds at the time of testing. Speed testing was carried out after calibrating and placing speed detectors as described in the Autoscope user manual. Autoscope speed testing results were, as expected, more accurate in the nearer lanes. As the distance from the camera increased error increased as well. The near lane returned a Pearson's R-value above 0.9. The middle and far lane errors resulted in reduced R-values of 0.85 and 0.73 respectively.

Queue length testing demonstrated great accuracy and promise for future application to work-zones. With an accuracy of over 96% and a MAPE under 4% this detection system

surpasses the expectations of the practitioners we consulted with. Queue length testing was carried out using a trip-wire based algorithm, which was compared once per cycle to a visual ground truth. The algorithm used took into account vehicle occupancy and demonstrated high accuracy at distances up to 450 feet.

Currently a new proprietary tracking algorithm is being considered for testing in an effort to increase accuracy. Furthermore, wireless transmission of streaming video from the box will be developed to allow for streaming video and traffic data. Such advances are ideal for use in conjunction with existing deployments of machine vision sensors at arterials.

References

[1] D. Panda, “An Integrated Video Sensor Design for Traffic Management and Control,” *Third International Multiconference on Circuits, Systems, Communications, and Computers*, pp. 4–8, 1999.

[2] MN/DOT, *NIT Phase II Evaluation of Non-Intrusive Technologies for Traffic Detection, Final Report*, MNDoT, Saint Paul, MN, 2002.

[3] P. Martin, Y. Feng, and X. Wang, *Detector Technology Evaluation*, University of Utah Traffic Lab., Salt Lake City, Utah, 2003.

[4] Miovision. "Automated Turning Movement Count System," February 2009, 2009; http://www.miovision.com.

[5] OMJC. "Super PJ, Waterloo, Iowa," July 15, 2009; http://www.omjcsignal.com/superpj.php.

[6] J. Hourdakis, P. Michalopoulos, and T. Morris, “Deployment of Wireless Mobile Detection and Surveillance for Data-Intensive Applications,” *Transportation Research Record,* vol. 1900, no. -1, pp. 140-148, 2004.

[7] J. Kotzenmacher, E. D. Minge, and B. Hao, *Evaluation of Portable Non-Intrusive Traffic Detection System,* Final Report MN-RC-2005-37, Mn/DOT, Saint Paul, MN, 2005.

[8] Y. BAI, Y. LI, and K. Lawrence, “Determining Major Causes of Highway Work Zone Accidents in Kansas,” *RE,* vol. 375, pp. 01.

[9] M. Fontaine, “Guidelines for Application of Portable Work Zone Intelligent Transportation Systems,” *Transportation Research Record,* vol. 1824, no. -1, pp. 15-22, 2003.

[10] C. Wang, K. Dixon, and D. Jared, "Evaluation of Speed Reduction Strategies for Highway Work Zones." pp. 2003-2099.

[11] P. Wiles, S. Cooner, C. Walters *et al.*, “Advance warning of stopped traffic on freeways: current practices and field studies of queue propagation,” *Texas Department of Transportation, Austin, TX, Research report FHWA/TX-03/4413-1, June*, 2003.

[12] L. Tudor, A. Meadors, and R. Plant, “Deployment of Smart Work Zone Technology in Arkansas,” *Transportation Research Record,* vol. 1824, no. -1, pp. 3-14, 2003.

[13] J. Sullivan, “Work-zone safety ITS: smart barrel for an adaptive queue-warning system,” 2005.

[14] MN/DOT, "Minnesota Manual on Uniform Traffic Control Devices," MN/DOT, Saint Paul, MN, 2005.

[15] Econolite. "RTMS G4," July 15, 2009; http://www.imagesensingca.com/en/RTMS/RTMSG4/tabid/65/Default.aspx.

[16] R. R. K. Andrew J Graettinger, Meghavardhan R. Govindu, Philip W. Johnson, S. Rocky Durrans, “Federal Highway Administration Vehcile Classification from Video Data and a Disaggregation Model,” *Journal of Transportation Engineering,* vol. September 2005, pp. 689-698, September 2005, 2005.

[17] MN/DOT. "Metro Warrants," May, 2007; http://www.dot.state.mn.us/metro/warrant/).

[18] J. Bonneson, and M. Abbas, *Intersection Video Detection Field Handbook*, College Station, TX: Texas Transportation Institute, Texas A&M, 2002.
[19] J. Kotzenmacher, E. D. Minge, and B. Hao, *Evaluation of Portable Non-Intrusive Traffic Detection System,* Final Report MN-RC-2005-37, Mn/DOT, Saint Paul, MN, September 2005.
[20] J. Schwach, and P. Michalopoulos, "Rapidly Deployable Low Cost Traffic Data and Video Collection Device," in ITS World Congress, Minneapolis, MN, 2008.
[21] P. Michalopoulos, "Vehicle detection video through image processing: the Autoscopesystem," *Vehicular Technology, IEEE Transactions on,* vol. 40, no. 1, pp. 21-29, 1991.
[22] MN/DOT. "Metro Intersection Warrant Information Website," November 2009, 2009; http://www.dot.state.mn.us/metro/warrant/index.html.
[23] M. Loeve, *Probability Theory*, 4 ed., p.^pp. 12: Springer-Verlaf, 1977.
[24] D. Moore, *Basic Practice of Statistics*, 4th ed., p.^pp. 90 - 114: WH Freeman Company, 2006.
[25] N. Nagelkerke, "A Note on a General Definition of the Coefficient of Determination," *Biometrika,* vol. 78, no. 3, pp. 691 - 692, 1991.
[26] P. Michalopoulos, R. Fitch, and M. Geokezas, *Development Of A Visible/Infrared Vehicle Detection System. Phase I: Feasibility Study*, University of Minnesota, Minneapolis, MN, 1986.
[27] Z. Tian, and M. Abbas, "Models for Quantitative Assessment of Video Detection System Impacts on Signalized Intersection Operations," *Transportation Research Record: Journal of the Transportation Research Board,* vol. 2035, no. -1, pp. 50-58, 2007.
[28] A. Tarko, and R. Lyles, *Development of a Portable Video Detection System for Counting Turning Vehicles at Intersections*, West Lafayette, Indiana: Purdue University, Joint Transportation Research Program, 2002.
[29] S. Mohan, and P. Gautam, "Cost of Highway Work Zone Injuries," *Practice Periodical on Structural Design and Construction,* vol. 7, pp. 68, 2002.
[30] H. Veeraraghavan, P. Schrater, and N. Papanikolopoulos, "Robust target detection and tracking through integration of motion, color, and geometry," *Computer Vision and Image Understanding,* vol. 103, no. 2, pp. 121-138, 2006.

Appendix

The following procedure was developed to extract turning movements and signal movement phases. In order to use the algorithm, each intersection is calibrated using a procedure, which utilizes directional detectors that are part of the current AutoScope detector suite.

Necessary Reading

- **Please read Autoscope help files on:**
  - **Edit Detectors (Detector Placement) Window**
  - **Calibration**
  - **Count Detectors**
  - **Presence Detectors (directional)**
  - **Station Detectors**
  - **Data Collector**

Procedures

1. Image and Calibration
2. Out Detector
3. Left Turn Detectors
4. Right Turn Detectors
5. Phase Functions
6. Straight Movement Functions
7. Right Turn Movement Functions
8. Left Turn Movement Functions
9. Phase Detectors
10. Data Collector

-

Image and Calibration Procedure

1. Open Detector Placement Window
2. Upload Image from Autoscope
3. Calibrate Image

Out Detector Procedure

1. Study the following images and comments for out detector placement techniques.

Place detectors through the middle body of near lanes to increase accuracy, while placing detectors near the top of occlusion prone lanes to minimize errors.

Out Detector Procedure Continued

Try to place detectors in areas of the lane that are not occlusion prone. Set placement based on normal vehicles like cars or vans, trucks and buses will always cause some problems but are often only a fraction of the vehicle volume. The above is a bad placement, the below is better.

Out Detector Procedure Continued

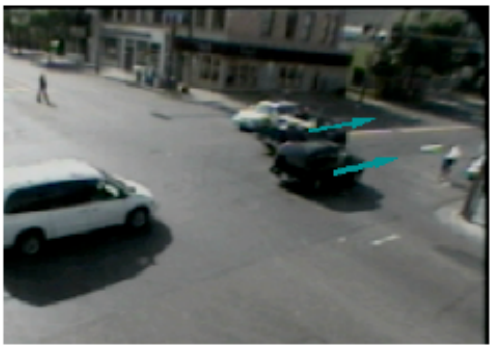

Occlusion as seen above is the reason for placing detectors in or beyond the crosswalk for Out Detectors, however, if placing detectors within the intersection in necessary or any reason, placing detectors such as to minimize occlusion is ideal (as seen above).

Out Detector Procedure Continued

To the left is a poor detector placement due to the excessive length of the detector. The detector is longer than the average vehicle gap at this area and thus will likely stay on and only count the two (or more) cars as one.

This is a much better detector placement.

Out Detector Procedure Continued

2. Place 'directional' presence detectors in or outside of crosswalks for each outbound *lane*. (no detector titles necessary)

- NOTE: Try to make the detectors short in length to minimize downlane occlusion.

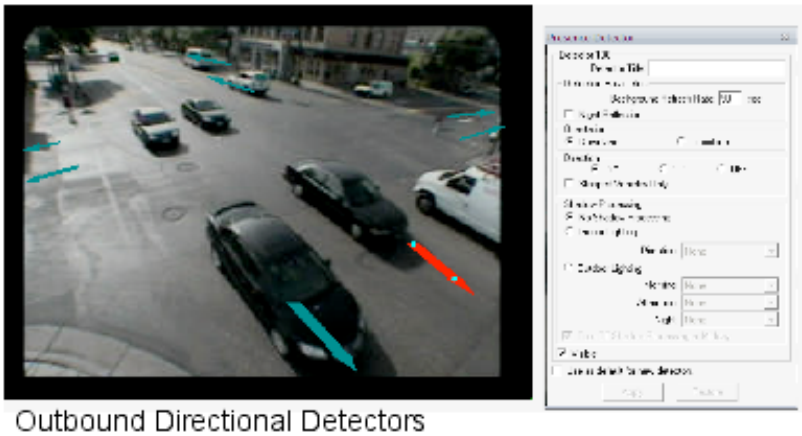

Outbound Directional Detectors

Out Detector Procedure Continued

3. Upload detector file to Autoscope and run to make sure the locations are ideal (ie: maximum accuracy and minimum occlusion)

- NOTE: If not yet accurate, alter placement of detectors as necessary and try again.

Left Turn Detectors Procedure

1. If the turn lane **IS a dedicated turn lane**, then place a directional detector over a small area (to prevent downlane occlusion) where the turning cars enter the intersection (and that at it).

Left Turn Detectors Procedure Continued

- Below is another proper detector placement (in red) for dedicated turn lanes. Make sure that the detector placement does not encounter occlusion that could trigger it (should be fine if properly placed based on techniques seen in the Out detector procedure.

-

Left Turn Detectors Procedure Continued

2. If the turn lane is **NOT a dedicated turn lane**, place directional detector over general path of turning movement

- (Do not worry about through cars from the far approach hitting this detector as it won't matter as long as perpendicular cars don't trigger it.)
- In order words, based on the below image, the car above the turn detector should NOT trigger the detector but the cars from the right moving left won't matter).

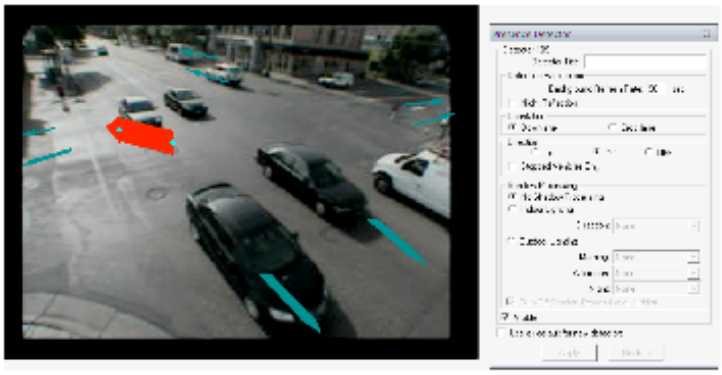

Left Turn Detectors Procedure Continued

- Below is the proper placement of a left turn detector is not a dedicated turn lane.
- Notice the thickness used to account for the variation in vehicle trajectories. (ctrl + down or up to change detector thickness; see help files for more)

3. Repeat for each left turn.

Right Turn Detectors Procedure

- NOTE: The right-most out lane detectors can be used as the right turn detectors instead of the following procedure for non-dedicated right turn lanes.

1. For **DEDICATED** turn lanes, in this case the right turning lane, a simple directional detector over a small area (to prevent downlane occlusion) where the turning cars enter the intersection is sufficient.
- (See image in step 1 of Left Turn Direction Detector Procedure)

Right Turn Detectors Procedure Continued

1. For **NON-DEDICATED** right turns, the right-most out lane detector can be used as the right turn detector or a detector similar to the left turn detector can be placed. See the below image.

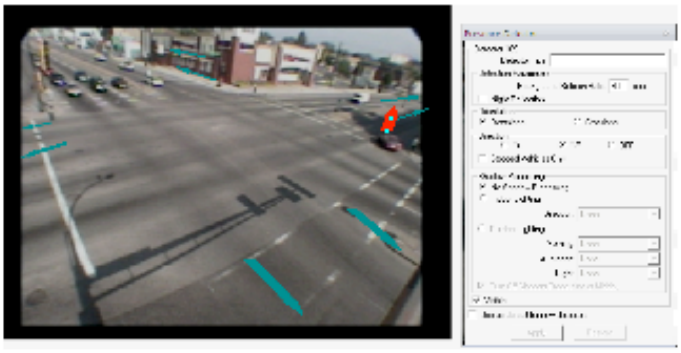

The above image shows a right turn detector where the option for turning right into a number of lanes makes the use of functions less desirable than placing a new right turn detector that is thicker and accounts for the potential trajectories of the turning c

Phase Function Procedure

1. For each approach a phase function is needed. This will be an And function for approaches will many lanes or large areas (will be explained later), or an OR function for approaches with fewer or small visible area.
2. Make a function for each approach
3. In the function parameters, add a 2.5 second extension.

Notice the 2.5 second extended time for the phase function.

Straight Movement Functions Procedure

1. Connect each out detector to the appropriate phase functions for each straight movement using an AND function (with no extended Time). Also Title these detectors with the first letter of the, from and to direction (for example: West to East→ WE). See the image below.

Straight Movement Functions Procedure Continued

The above image shows how the West to East straight functions should look.

Notice the AND Boolean logic function and the "WE" in the detector title for West to East – (repeat in similar fashion for each approach).

2. Repeat for all straight movements

Right Turn Movement Functions

1. Connect each out detector to the appropriate phase functions for each right turn movement using an AND function (with no extended-Time). Also Title these detectors with the first letter of the, from and to direction (for example: West to South→ WS). See the image below.

Right Turn Movement Functions Continued

Above is the proper setup of the right turn function for use with existing out detectors; else see below for separate (optional) right turn detector setup with the right turn function. Notice the WS in the detector title and the AND in the operation type.

Right Turn Movement Functions Continued

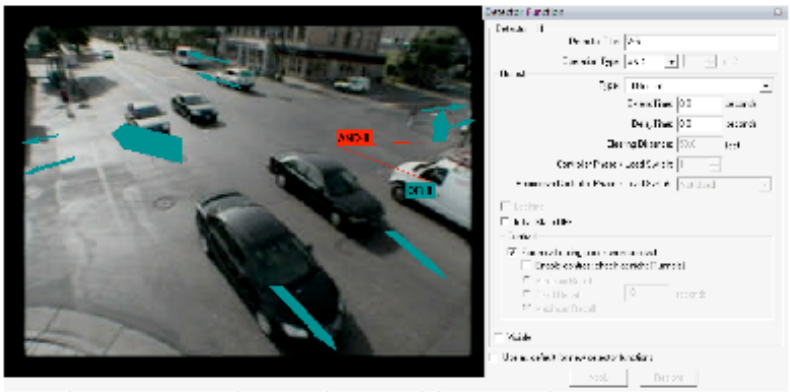

Above is the proper setup for the right turn function given a separate right turn detector. This function has the same parameters as the right turn function parameters with the non-separate right turn detector.

2. Repeat for all right turn movements

Left Turn Movement Functions Procedure

Connect each left turn detector to the appropriate phase functions for each left turn movement using an AND function (with no extended Time). Also Title these detectors with the first letter of the, from and to direction (for example: West to North → WN). See the image below.

Left Turn Movement Functions Procedure Continued

Below is the proper parameters and setup for the left turn function. Again, notice the AND in the operation type and the WN in the detector title.

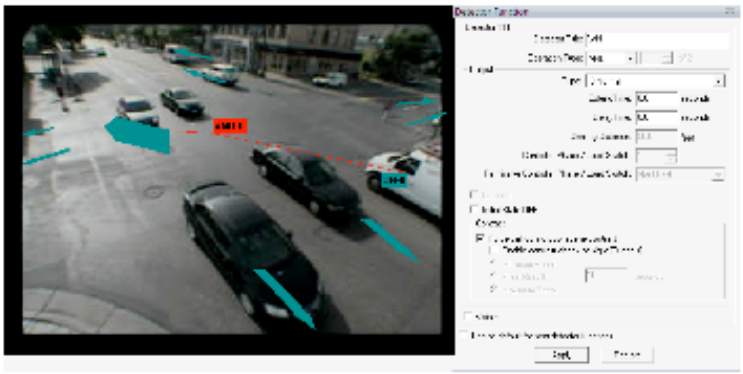

2. Repeat for all left turn movements

Phase Detectors Procedure

NOTE: These detectors will be the member for the phase functions created earlier. So once the detectors are setup, add them as members to the corresponding phase functions.

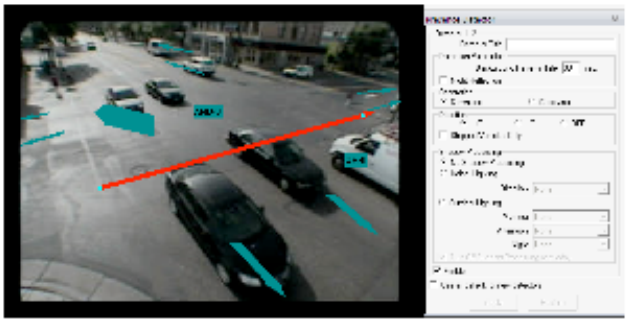

1. Create phase detectorsfor each approach. These detectors should go from the inner crosswalk line to the far crosswalk (inner-most) line on the other side of the intersection. After placing and thickening each of these detectors, add more detectors in the same manner until the entire approach area is covered. (NOTE: the phase function will need to be an AND function if one than one of these detectors is needed on a given approach.
   See the images that follow.

Phase Detectors Procedure Continued

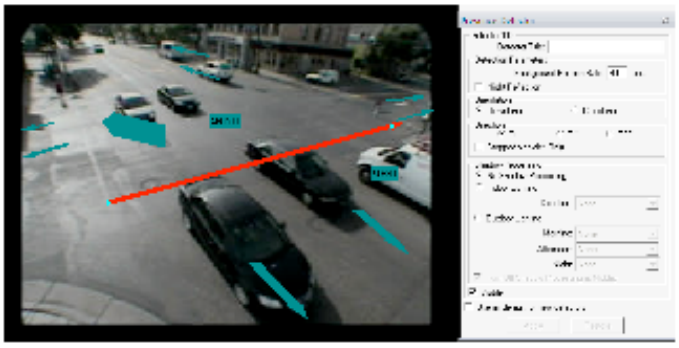

Notice how the phase detector extends from the near inner-crosswalk line to far inner-crosswalk line.

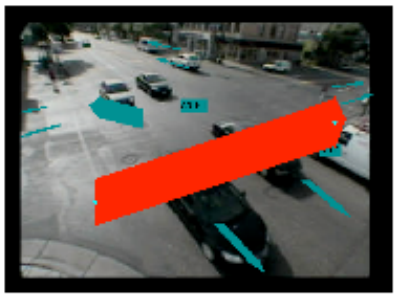

The detector lines were not only made thick as possible but placed in such a way as to allow a second phase detector to be placed to cover all possible approaching cars. (see next image)

Phase Detectors Procedure Continued

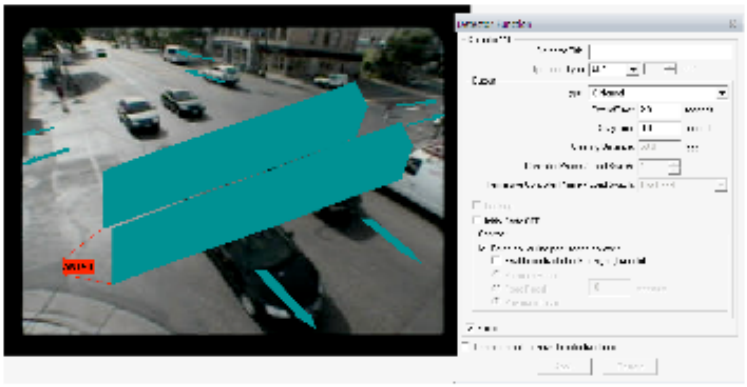

Above shows the entire approach being covered by two phase detectors (always made as thick as possible without leaving the approach), and the function now becoming an AND operation type with both of the phase detectors as members.

Phase Detectors Procedure Continued

2. Repeat for each approach

NOTE: Trial and error may be needed to ensure that all approaching cars are picked up by the appropriate and only the appropriate phase detectors.